Document Room, DOCUMENT ROOM 36-412
Research Laboratory of Electronics
Massachusetts Institute of Technology

#1

HIGH-FREQUENCY GAS-DISCHARGE BREAKDOWN

SANBORN C. BROWN

LOAN COPY
only

TECHNICAL REPORT 301

JULY 25, 1955

RESEARCH LABORATORY OF ELECTRONICS
MASSACHUSETTS INSTITUTE OF TECHNOLOGY
CAMBRIDGE, MASSACHUSETTS

The Research Laboratory of Electronics is an interdepartmental laboratory of the Department of Electrical Engineering and the Department of Physics.

The research reported in this document was made possible in part by support extended the Massachusetts Institute of Technology, Research Laboratory of Electronics, jointly by the Army Signal Corps, the Navy Department (Office of Naval Research), and the Air Force (Office of Scientific Research, Air Research and Development Command), under Signal Corps Contract DA36-039 sc-42607, Project 132B; Department of the Army Project 3-99-12-022.

MASSACHUSETTS INSTITUTE OF TECHNOLOGY

RESEARCH LABORATORY OF ELECTRONICS

Technical Report 301 July 25, 1955

HIGH-FREQUENCY GAS-DISCHARGE BREAKDOWN

Sanborn C. Brown

This report is identical with material prepared
for Handbuch der Physik, Volume XXII, 1955.

Abstract

In this report an attempt is made to summarize our knowledge of high-frequency gas-discharge breakdown. The types of processes discussed include diffusion-controlled, mobility-controlled, and electron-resonance breakdown, as well as breakdown phenomena in the presence of magnetic and dc electric field superimposed on the high-frequency electric field.

TABLE OF SYMBOLS

α - first Townsend ionization coefficient (cm^{-1})

B - magnetic field (gauss)

β - attachment frequency

C - collision source term

c - velocity of light

D - diffusion coefficient

E - rms electric field

e - $+1.6 \times 10^{-19}$ coulomb

F - distribution function

f - energy dependent part of F

Γ - electron flow density

η - ionization coefficient ($volt^{-1}$)

J - electron current density

L - parallel-plate separation

ℓ - mean free path

Λ - characteristic diffusion length

λ - wavelength

M - mass of gas atom or molecule

m - mass of electron

μ - mobility

N - total number of collisions during an electron lifetime

n - electron density

ν - collision frequency

ω - radian frequency

P - power and probability of collision

p - pressure (mm Hg)

q - appearance frequency

R - radius

S - source function

u - energy

v - velocity

ζ - ac ionization coefficient

SUBSCRIPTS

b - cyclotron

c - collision

e - effective

i - ionization

m - momentum transfer

p - peak

x - excitation

A. DIFFUSION CONTROLLED BREAKDOWN

I. Behavior of the Average Electron

1. General Considerations

In an ultra-high-frequency gas discharge breakdown, the primary ionization from the electron motion is the only production phenomenon that controls the breakdown, and for this reason it is the simplest type to consider. If one calculates the maximum kinetic energy in the oscillatory motion of an electron at the minimum field intensities for breakdown experimentally determined, one finds that this energy corresponds to about 10^{-3} volt. It is therefore obvious that the energy of oscillation is insufficient to account for breakdown.

It is well known that a free electron in a vacuum under the action of an alternating field oscillates with its velocity 90° out of phase with the field in the steady state, and thus takes no power, on the average, from the applied field. The electron can gain energy from the field only by suffering collisions with the gas atoms, and it does so by having its ordered oscillatory motion changed to random motion on collision. The electron gains random energy, on the average, on each collision until it is able to make an inelastic collision with a gas atom. The electron continues to gain energy in the field, on the average, despite the fact that it may either move with or against the field. The energy absorbed is proportional to the square of the electric field and hence independent of its sign. The rate of gain of energy of the electron from the electric field E is $P = (-eE_p v_p)_{real}/2$. We may express the average drift velocity v in terms of the ac mobility in the following way. Writing Newton's second law for the motion of the electrons in the form

$$m\,(dv/dt) + (m\nu_m)\,v = -eE_p \exp(j\omega t), \tag{1.1}$$

the velocity may be determined as

$$v = -\left[e/(j\omega m + m\nu_m)\right] E_p \exp(j\omega t) \tag{1.2}$$

and ν_m is the collision frequency for momentum transfer. Thus the ac mobility takes the form $\mu = -e/(j\omega m + m\nu_m)$. We may write for the power absorbed by the electrons from the ac electric field:

$$P = ne\mu E^2_{real} = \frac{ne^2E^2}{m\nu_m}\left(\frac{\nu_m^2}{\nu_m^2 + \omega^2}\right), \quad E^2 = \frac{E_p^2}{2}. \tag{1.3}$$

This equation may be written in terms of an effective field E_e:

$$P = \frac{ne^2E_e^2}{m\nu_m}, \tag{1.4}$$

where E_e is the effective field that would produce the same energy transfer as a steady field and is given by

$$E_e^2 = E^2 \frac{\nu_m^2}{\nu_m^2 + \omega^2} . \tag{1.5}$$

The gas discharge breakdown occurs when the gain in electron density resulting from ionization of the gas becomes equal to the loss of electrons by diffusion, recombination, or attachment. When the loss is by diffusion, the problem becomes simple. We shall discuss this case first.

Diffusion occurs whenever a particle concentration gradient exists. The total flow of particles out of a volume of high concentration may be written from ordinary kinetic theory considerations as

$$\underline{\underline{\Gamma}} = -D\nabla n, \tag{1.6}$$

where D is the diffusion coefficient for electrons, n is the electron density, and $\underline{\underline{\Gamma}}$ is the electron flow density in electrons per second per unit area.*

We shall develop the breakdown conditions for a region bounded by walls that absorb electrons. A radioactive source near the discharge tube provides a small amount of ionization S in the tube. A detailed study of the build-up of the discharge is obtained from considering the continuity equation for electrons

$$\partial n/\partial t = \nu_i n + S - \nabla \cdot \underline{\underline{\Gamma}} \tag{1.7}$$

or

$$\partial n/\partial t = D\nabla^2 n + \nu_i n + S. \tag{1.8}$$

In Eq. 1.8 the term $D\nabla^2 n$ describes the loss of electrons by diffusion. The term $\nu_i n$ is the rate of gain of electrons by ionization; S is the rate at which electrons are produced by an external source. For the case of infinite parallel plates

$$\partial n/\partial t = D(\partial^2 n/\partial x^2) + \nu_i n + S. \tag{1.9}$$

Assuming that the approach to breakdown is so slow in time that $\partial n/\partial t$ may be neglected,

$$-S = D(\partial^2 n/\partial x^2) + \nu_i n. \tag{1.10}$$

This is a characteristic value problem which may be solved under the conditions that S, D, and ν_i are uniform throughout the cavity and that the boundary condition on the electron density is zero at the walls. Rigorous boundary conditions require the concentration to be small at a boundary and to extrapolate to zero outside the boundary at

*In this report vectors are indicated by double underline.

a distance of the order of a mean free path. In the range of pressures to be considered, the mean free path is very small compared to cavity dimensions, and the condition of zero concentration on the cylinder walls is imposed. The solution of Eq. 1.10 tells us that the electron density just before breakdown, at any distance x from the median plane between parallel plates of separation L, may be written

$$n = (4S/\pi)\cos(\pi x/L)/\left[D(\pi/L)^2 - \nu_i\right]. \tag{1.11}$$

Breakdown can be defined by the condition that the electron density goes to infinity, which occurs when $\nu_i = D(\pi/L)^2$.

If we write $\nu_i/D = (\pi/L)^2 = 1/\Lambda^2$, for parallel plates, the quantity Λ is known as the characteristic diffusion length and is very useful in describing the shape of the gas container when discussing diffusion problems. One other example of a very useful boundary condition is the case of a cylinder of height L and radius R, with flat ends. This geometry leads to the relation that $1/\Lambda^2 = (\pi/L)^2 + (2.4/R)^2$, where the diffusion to the end plates is given by the first term on the right; the second term describes the diffusion to the cylindrical walls.

2. Ionization Coefficients

Gas-discharge phenomena under the action of dc fields are often described in terms of Townsend ionization coefficients. If one considers that electrons in a dc field create α new electrons in a path one centimeter long in the field direction, the increase of electrons, dn, produced by n electrons in a distance dx will be $dn = \alpha n\, dx$, and $n = n_o e^{\alpha x}$, where n_o is the initial electron concentration. The quantity α is called the first Townsend coefficient. This first Townsend coefficient may also be written as the ionization produced by an electron falling through a potential difference of one volt rather than traveling one centimeter. This coefficient is given the symbol η and is related to α by $\eta = \alpha/E$.

These Townsend first ionization coefficients may be given in terms of an "ionization" collision frequency. Since α is the number of electrons produced by the collisions of the primary electrons traveling one centimeter, one can write $\alpha = \nu_i/v$, where ν_i is the frequency of ionization, and v is the average drift velocity of the electrons in the field. The average drift velocity $v = |\mu E|$, and one may write $\alpha = \nu_i/\mu E$ or

$$\eta = \nu_i/\mu E^2. \tag{2.1}$$

By analogy with the first Townsend coefficient for dc ionization, where the electron loss is controlled by mobility, we may define a coefficient for high-frequency discharges, where the loss is by diffusion, as

$$\zeta = \nu_i/DE_e^2. \tag{2.2}$$

From our previous discussion of diffusion we saw that at breakdown $\nu_i/D = 1/\Lambda^2$. Thus we may measure the ac ionization coefficient by measuring the breakdown field in tubes of known size, since $\zeta = 1/\Lambda^2 E_e^2$.

There is a very close physical relation between the ac and the dc ionization coefficients. If one divides Eq. 2.1 by Eq. 2.2, there results the relation $\eta/\zeta = D/\mu$. Townsend showed that the ratio of D/μ was a measure of the average energy of the electrons and determined this average energy as a function of E/p experimentally. Thus, in principle, one can determine η from ζ, or vice versa, from these Townsend-like measurements. There is difficulty in carrying this out exactly, however, because the actual values depend on the manner in which the averaging of the energy is carried out. Since the electron energy-distribution functions are different for the ac and the dc cases, one might expect mathematical complications to arise. However, in the two cases[1, 2] in which distribution function calculations have connected the dc and ac ionization coefficient, very satisfactory results have been obtained.

3. Breakdown Fields

Typical of the behavior of the breakdown field at high frequency with changes in gas pressure are the curves shown in Fig. 1. At first sight these curves look similar to corresponding data taken with dc fields, that is, as the pressure is decreased the breakdown field first decreases and then increases again at low pressures. In the low-pressure region, the rising breakdown field with decreasing pressure in high-frequency discharges corresponds to the increasing loss of efficiency in the transfer of energy from the field to the electrons. We saw in the introduction that the electron only gained energy insofar as it made collisions with the gas atoms and that between collisions it oscillated out of phase with the field and hence gained no energy. Thus, as the pressure is reduced, one must increase the field to make up for the loss of efficiency by just the factor of the effective field given in Eq. 1.5. In the high-pressure region, the reason for the rising breakdown field with increasing pressure in high-frequency discharges is the same as in the dc case. As the pressure increases, the electron mean free path decreases, and the energy gained per mean free path decreases as the square of the mean free path--as can be seen from Eq. 1.4. Since at these high pressures, most of the energy losses result from recoil losses in collision with the gas molecules, and the average electron energy is practically independent of the pressure, the energy gain per mean free path is proportional to the mean free path at constant E field. The field must increase inversely proportionally to the mean free path, or directly proportionally to the pressure. The minimum corresponds essentially to the point at which the frequency of collision between electrons and gas atoms is equal to the frequency of the applied rf field. Thus at low pressure, where the electron makes many oscillations per collision, its

1. S. Krasik, D. Alpert, A. O. McCoubrey, Phys. Rev. 76, 722 (1949).
2. L. J. Varnerin, S. C. Brown, Phys. Rev. 79, 946 (1950).

behavior is governed by strictly ac considerations. At high pressure, where the electrons make many collisions per oscillation, their behavior is the same as in a dc discharge.

The remarkable feature of the breakdown curves, for those used to dc phenomena, is the fact that the greater the electrode spacing, the easier it becomes to cause a breakdown. This, of course, is a necessary result of the breakdown condition of the balance between energy gained from the field and electron loss by diffusion. As the electrode spacing becomes less, the diffusion loss becomes greater; therefore, the field must increase to make up for the increased loss.

Curves of gas-discharge breakdown as a function of pressure are often plotted in dc work as Paschen curves in which, for a particular gas, the breakdown voltage V is found to be a function of pd independent of the magnitude of the electrode spacing d. The same type of quantities may be introduced in the high-frequency case, where for the breakdown voltage we write $E\Lambda$, the product of the field and the diffusion length, and for pd we use $p\Lambda$. In the case of high-frequency phenomena we have one more variable than for the dc case, namely, the frequency, and this may be introduced as the variable $p\lambda$, where λ is the wavelength of the applied field. However, if we express the electric field in terms of its effective value E_e, we can take care of the frequency variations. The effective field is strictly correct only when ν_m is constant, but a similar equation would be valid for different variations of ν_m with energy. With $E_e\Lambda$ (the breakdown voltage) plotted as a function of $p\Lambda$, experimental results for ultra-high-frequency breakdown are shown in Fig. 2.

The simplest gas to discuss theoretically is helium containing small admixtures of mercury vapor. This mixture, which for convenience we call Heg gas, has the advantage of acting as a gas of atoms without excitation levels. Helium has a metastable level at 19.8 volts, and transitions from this level to the ground state by radiation are forbidden. Since the metastable states have mean lives of the order of thousands of microseconds, practically every helium atom which reaches an energy of 19.8 volts will collide with a mercury atom and lose its energy by ionizing the mercury. Therefore, each inelastic collision will produce an ionization, and the effective ionization potential will be $u_i = 19.8$ volts. Furthermore, for Heg the collision frequency may be considered constant, having a value $\nu_m = 2.37 \times 10^9 p$.

Although an accurate description of the breakdown measurements can be given theoretically only by taking into account the electron energy distribution, a physical picture of the mechanisms involved can be seen qualitatively in the following way. Let us consider a gas at high pressure. The power that goes into the electron from the electric field is dissipated in elastic collisions between the electrons and the gas molecules. For this case

$$\text{energy/collision} = \frac{e^2E^2}{m\nu_m^2} = e\,\frac{2m}{M}\,\bar{u} \tag{3.1}$$

where $\bar{u}$ is the average energy. From this we may calculate the electric field to be

$$E = \left(\frac{m}{e}\frac{2m}{M}\bar{u}\right)^{1/2} \cdot \nu_m = 0.94\, p(\bar{u})^{1/2} \tag{3.2}$$

for the case of Heg gas in which nearly all the loss goes into non-ionizing collisions. Taking the average energy equal to one-third of the ionization potential, $E = 2.4\, p$. It can be seen that the high-pressure breakdown measurements of Fig. 1 tend to approach this line at high pressures.

In the low-pressure region, the electrons make many oscillations per collision and the breakdown field may be determined by equating the number of collisions to ionize to the number of collisions to diffuse out of the tube. Since we are discussing Heg gas, where all of the inelastic collisions are ionizing ones, let us consider that all of the input power goes into ionization, and write

$$\nu_i = \frac{P}{eu_i} = \frac{eE^2}{mu_i\nu_m}\left(\frac{\nu_m^2}{\nu_m^2 + \omega^2}\right). \tag{3.3}$$

The breakdown condition is $\nu_i = D/\Lambda^2$, and substituting the value of the diffusion coefficient $D = \ell\bar{v}/3$ we find $\nu_i = \ell\bar{v}/3\Lambda^2$. If we multiply the numerator and the denominator of this expression by the velocity, we obtain an expression in terms of the average energy which we may set equal to the previous expression for ν_i, in which $\omega^2 >> \nu_m^2$, to obtain

$$\nu_i = \frac{\bar{v}^2}{3\Lambda^2\nu_m} = \frac{eE^2\nu_m}{u_i m\omega^2}. \tag{3.4}$$

If we solve this expression for the electric field, writing ω in terms of λ and $2\bar{u} = m\bar{v}^2/e$, we get

$$E = \frac{2\pi c}{\Lambda\lambda\nu_m}\left(\frac{2}{3}\bar{u}u_i\right)^{1/2}. \tag{3.5}$$

The ionization potential is 19.8 volts, and we assume a very low pressure, where all of the input power goes into ionization, and the average energy is of the order of the ionization potential. Calculating the electric field under these approximations leads to a relation $E = 1284/p\Lambda\lambda$, which agrees fairly well with the low-pressure measurements shown in Fig. 1.

4. Proper Variables

If a gas contained in a vessel is placed in an alternating electric field, for a certain value of the electric field the gas will break down into an electrical discharge. This breakdown field may be expressed as

$$E_b = E(u_i, \Lambda, \lambda, p), \tag{4.1}$$

The term Λ has the units of length, and its appearance in explicit calculations also involves various known dimensionless ratios describing the shape of the vessel. It is customary to measure pressure in millimeters of mercury; the mean free path, which is inversely proportional to pressure, is measured in centimeters. A relation between pressure and mean free path is obtained by introducing the quantity, P_m, which is the number of collisions per unit length at a pressure of 1 mm Hg. Thus, P_m may be regarded as having the units of reciprocal length, even though this is not its true dimension.

Treating the breakdown problem dimensionally, there are five variables with but two fundamental dimensions: volts and centimeters. This leads to three independent dimensionless variables between which there is a functional relation.[1] It is often convenient in physical problems to introduce variables that are not dimensionless but are, nevertheless, proper variables for dimensional analysis because the completely dimensionless variables contain one or more physically invariant quantities that need not be carried along in a practical discussion. There are a number of sets of such proper variables in a gas discharge problem that may be transformed into one another, and their relative convenience depends on the purpose for which they are to be used.

One very useful set of proper variables is

$$E\Lambda,\ p\Lambda,\ p\lambda. \tag{4.2}$$

The advantage of these variables lies in the fact that p, Λ, and λ are the experimentally independent parameters that determine the dependent variable E, the observed breakdown field.

Another set of proper variables that we shall use is obtained by dividing the first variable by the second and obtaining

$$E\Lambda,\ E/p,\ p\lambda. \tag{4.3}$$

This set has the particular advantage, in a discussion of breakdown phenomena, that we may define the ac ionization coefficient, $\zeta = 1/E^2\Lambda^2$, which is a function of E/p and $p\lambda$.

For the cases of a dc field, or when the pressure is high, so that in an ac field the electrons make many collisions per oscillation, the wavelength variation does not enter as a significant variable. Breakdown can then be described by the other two variables, such as $E\Lambda$ and $p\Lambda$, as illustrated in Fig. 2.

5. Limits of Diffusion Theory

Certain basic assumptions are made in the calculations of breakdown as a balance between the ionization rate and the loss of electrons by diffusion. We examine here the limits which the assumptions place on the application of the theory to various experimental conditions.[2] These limits can be discussed in terms of the proper independent

1. P. W. Bridgeman, "Dimensional Analysis," New Haven (1922), Chap. 4.
2. S. C. Brown, A. D. MacDonald, Phys. Rev. 76, 1629 (1949).

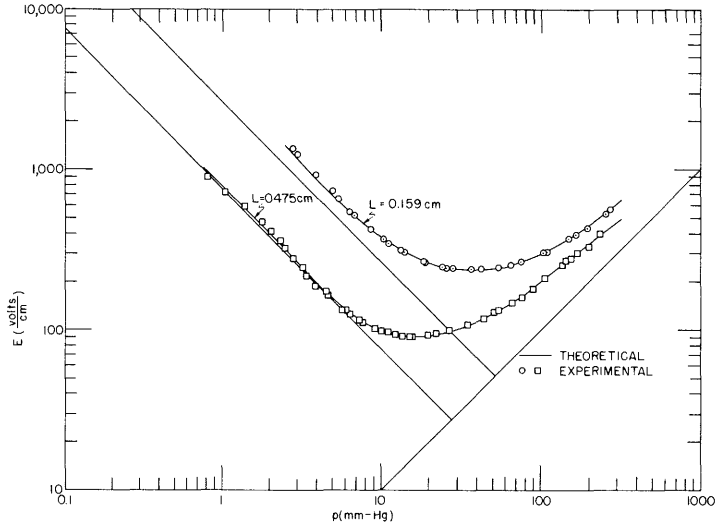

Fig. 1. Experimental breakdown electric fields compared with a simplified theory

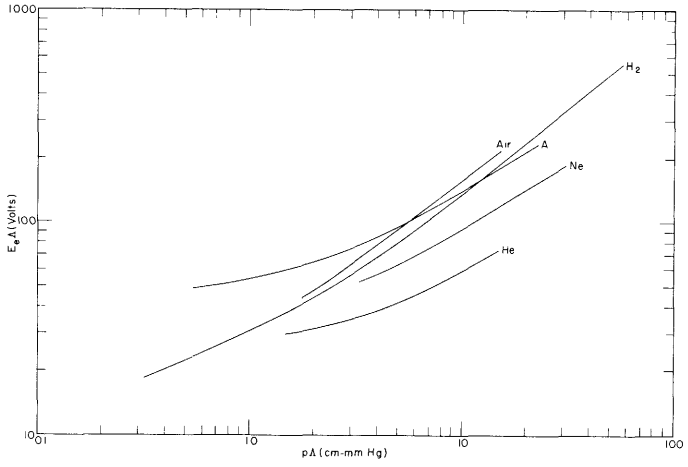

Fig. 2. Paschen curves for high-frequency breakdown

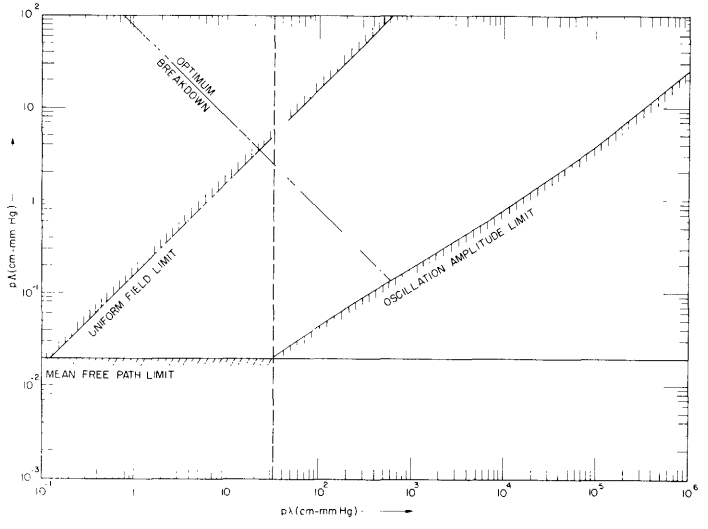

Fig. 3. Plot of the limits of the diffusion theory for breakdown of high frequencies in terms of variables derived from dimensional analysis

variables, $p\Lambda$ and $p\lambda$. One can plot on the $p\Lambda$-$p\lambda$ plane the conditions for all breakdown data for a single gas and derive limits in these variables which will define the applicability of the diffusion theory.

At low frequencies, the experimental measurements of breakdown are always taken in vessels whose dimensions are small compared to a wavelength of the exciting power. For this case, the uniform field assumption may be very good. At very high frequencies, there exists a limit to the size of the discharge tube consistent with the uniform field assumption of the diffusion theory. This limit can be written in terms of the size of vessel allowable to sustain a single loop of a standing wave of the electric field. The relation between the parallel plate separation, the wavelength, and the diffusion length may be written as

$$\frac{\lambda}{2} = L = \pi\Lambda . \tag{5.1}$$

Thus one arrives at a limit that can be written in terms of $p\lambda$ and $p\Lambda$ as

$$p\lambda = 2\pi(p\Lambda). \tag{5.2}$$

This limiting line is plotted in Fig. 3 and designated the Uniform Field Limit.

The diffusion theory will not apply if the electron mean free path becomes comparable to the tube size. In the limiting case, this can be expressed as the mean free path, ℓ, being equal to Λ. The probability of collision, P_m, is equal to $1/p\ell$. To plot this condition in Fig. 3 we may write

$$p\Lambda = 1/P_m . \tag{5.3}$$

The value of P_m is not a constant, but depends upon the electron energy. If we assume that the average electron has an energy equal to one-third of the ionization potential, the average electron energy would be 5 volts for hydrogen. Using measured values for the probability of collision in hydrogen for the average electron, we get $P_m = 49\,(\text{cm-mm Hg})^{-1}$. With this value, we obtain the horizontal line in Fig. 3 marked Mean Free Path Limit.

Within the limits of experimental conditions in which diffusion theory adequately explains the breakdown behavior, several different phenomena may occur. One of the phenomenological changes that is important is the transition from many collisions per oscillation of the electron to many oscillations per collision. This can be written as the condition that $\nu_m = \omega$, where ν_m, the collision frequency, is the ratio of the average velocity v to the mean free path, and ω is the radian frequency of the applied field. Using a value of the collision frequency, $\nu_m = 5.93 \times 10^9 p$, and putting this in terms of the proper variables, we obtain

$$p\lambda = 32. \tag{5.4}$$

This relation is plotted in Fig. 3 as the dotted line marked Collision Frequency Transition.

We can calculate a line on the $p\Lambda$-$p\lambda$ plane corresponding to the minimum breakdown field for any given container size. At low pressure we have seen that the breakdown field approaches the condition that $E = 2\pi c(2\bar{u}u_i/3)^{1/2}/\Lambda\lambda\nu_m$. For hydrogen, $\nu_m = 5.93 \times 10^9 p$, $u_i = 15.4$ volts, and we consider $\bar{u} = u_i$. This leads to a value of $E = 400/\Lambda\lambda p$. Using Eq. 3.2 for hydrogen leads to $E = 5.3p$. Eliminating the field between these two equations will allow us to calculate the pressure at which breakdown will occur most easily. In terms of the variables of Fig. 3 this leads to the equation

$$p\lambda = \frac{75}{p\Lambda}. \tag{5.5}$$

This relation is plotted in Fig. 3 as the line marked Optimum Breakdown.

When the amplitude of the electron oscillation in the electric field is sufficiently high, the electrons can travel completely across the tube and collide with the walls on every half-cycle.

Integrating Eq. 1.2, we obtain the displacement of the electron oscillation:

$$x = \frac{eE_p \exp(j\omega t)}{j\omega(j\omega + \nu_m)m}. \tag{5.6}$$

The amplitude of the oscillation is

$$\frac{eE_p}{m\omega\sqrt{\omega^2 + \nu_m^2}} = \frac{\sqrt{2}\, eE_e}{m\omega\nu_m}.$$

The limiting case on the diffusion mechanism in which all of the electrons will hit the walls would be calculated by setting the oscillation amplitude equal to one-half of the electrode separation. Thus, the oscillation amplitude limit becomes equal to

$$\frac{\sqrt{2}\, eE_e}{m\omega\nu_m} = \frac{L}{2}. \tag{5.7}$$

Substituting λ in terms of ω, v/ℓ in place of ν_m, and $1/pP_m$ for ℓ, we obtain

$$p\lambda = \left(\frac{\pi mc}{e} vP_m\right) \frac{pL}{\sqrt{2}\,(E_e/p)}. \tag{5.8}$$

Putting in numerical values and using the parallel plate relation that $L = \pi\Lambda$, one has

$$p\lambda = 10^6 \left(\frac{p\Lambda}{E_e/p}\right). \tag{5.9}$$

This equation can be solved numerically if the experimental values of the breakdown field are available. Experiments of this sort have been carried out for parallel-plate geometry with hydrogen gas, and numerical values can therefore be determined. This

calculation yields the Oscillation Amplitude Limit of Fig. 3. On crossing the amplitude of oscillation limit new mechanisms occur; they will be discussed in Chapter C.

II. Theories Based on the Boltzmann Transport Equation

a. High-Frequency Electric Fields

Up to this point we have discussed the phenomena associated with breakdown from the point of view of the behavior of the average electron. This presents a simple physical picture of breakdown, but does not give us a reliable mathematical basis for theoretical prediction of the behavior of the gas. We therefore turn to a more exact description of breakdown, restricting our discussion to those gases in which diffusion is the sole loss mechanism for electrons. First let us work out a fairly simple solution[1] applicable to any gas and a wide pressure range, and then discuss the specific problems that arise for individual gases.

6. Boltzmann Equation

When a high-frequency electric field, $E = E_p \exp(j\omega t)$, is applied to a gas, the velocity distribution $F(\underline{\underline{v}}, \underline{\underline{r}})$ of the free electrons is determined by the Boltzmann equation:

$$(\partial F/\partial t) = C - \underline{\underline{\nabla}}_r \cdot \underline{\underline{v}} F + \underline{\underline{\nabla}}_v \cdot e\underline{\underline{E}} F/m \tag{6.1}$$

where C represents the effect of collision, and ∇_r and ∇_v are the gradient operators in configuration and velocity spaces. This equation is solved by expanding the distribution function in spherical harmonics in velocity space and in Fourier series in time[2]:

$$F = \sum_{\ell} \sum_{k} F_k^{\ell} P_{\ell} (\cos\theta) \exp(jk\omega t)$$

$$= F_o^o + \underline{\underline{v}} \cdot \left[\underline{\underline{F}}_o^1 + \underline{\underline{F}}_1^1 \exp(j\omega t)\right]/v. \tag{6.2}$$

All terms except the three indicated may be dropped[3] when the geometry, pressure, and frequency fall within the limits discussed in Section 5. These limits require that the mean free path be less than any dimension of the cavity, that the frequency be sufficiently high so that the electrons do not lose appreciable energy between cycles, and that the average motion of the electrons resulting from the action of the field and of collisions be sufficiently small so that the field does not clear the electrons out of part

---

1. W. P. Allis, S. C. Brown, Phys. Rev. 87, 419 (1952).

2. For the mathematical details refer to W. P. Allis, "Motion of Ions and Electrons," Technical Report 299, Research Laboratory of Electronics, M.I.T., hereafter referred to as Allis.

3. Allis, Eqs. 19.2, 23.1. For the justification for dropping F_1^o see Allis, paragraph preceding Eq. 24.12.

of the tube in each half-cycle.

In evaluating the collision term it is convenient to replace the customary mean free paths by the collision frequencies for momentum transfer, for excitation, and for ionization defined by

$$\nu_m = \int\int vpP_m(\theta)(1 - \cos\theta)\sin\theta d\theta d\phi, \tag{6.3}$$

$$\nu_x = vpP_x, \quad \nu_i = vpP_i, \tag{6.4}$$

where P_x and P_i are the experimentally defined probabilities of excitation of all levels and of ionization, and $P_m(\theta)$ is the probability of scattering into a unit solid angle inclined at θ to the original direction.[1]

If the temperature of the gas is negligible compared to that of the electrons, the latter will lose a fraction 2m/M of their energy, per momentum transfer collision, to recoil of the molecule with which they collide. The mass of the molecule is M and that of the electron m. This fraction will be increased if there is appreciable transfer of energy to rotation or vibration but here it is assumed to be negligible.

A collision producing electronic excitation differs from that producing recoil, rotation, and vibration in that the colliding electron loses practically all of its energy instead of a very small fraction of it. These processes are treated mathematically as though fast electrons disappeared at the rate $(\nu_x + \nu_i)F_o^o$, and slow electrons appeared at the rate qF_o^o. Making use of these ideas in the evaluation of the collision term, introducing Eq. 6.2 into Eq. 6.1, and equating coefficients of similar time and angle functions yields one scalar and two vector equations:

$$(\nu_x + \nu_i - q)F_o^o = -(v/3)\,\underline{\underline{\nabla}}_r \cdot \underline{\underline{F}}_o^1 + (1/v^2) \times \partial\left[(ev^2/6m)\left(\underline{\underline{E}}_p \cdot \underline{\underline{F}}_1^1\right)_{real} + (m/M)\,\nu_m v^3 F_o^o\right]\Big/\partial v, \tag{6.5}$$

$$\nu_m \underline{\underline{F}}_o^1 = -v\,\underline{\underline{\nabla}}_r F_o^o, \tag{6.6}$$

$$(\nu_m + j\omega)\underline{\underline{F}}_1^1 = (e\underline{\underline{E}}_p/m)\,\partial F_o^o/\partial v. \tag{6.7}$$

7. Distribution in Space

The direct and alternating current densities,

$$\underline{\underline{J}}_o = \int_0^\infty -e\underline{\underline{F}}_o^1(4\pi v^3/3)\,dv = e\underline{\underline{\nabla}}_r Dn, \tag{7.1}$$

1. In this article, ν_m is the same as Allis' ν_{c1}, later simplified there to ν_c. See Allis, Eqs. 27.5-27.8 and associated discussion.

$$\underline{\underline{J}}_1 = \int_0^\infty - e\underline{\underline{F}}_1^1 (4\pi v^3/3)\,dv = e\mu\underline{\underline{E}}n, \tag{7.2}$$

are fully determined by the components $\underline{\underline{F}}_o^1$ and $\underline{\underline{F}}_1^1$ of the distribution function. These are, in turn, found to be derivatives of F_o^o. Substitution of Eqs. 6.6 and 6.7 into Eqs. 7.1 and 7.2 serves to determine the diffusion and ac mobility coefficients in terms of F_o^o:

$$nD = \int_0^\infty \frac{v^2}{3\nu_m} F_o^o\, 4\pi v^2 dv, \tag{7.3}$$

$$n\mu = \int_0^\infty \frac{4\pi}{3}\frac{e}{m} F_o^o \frac{d}{dv}\left(\frac{v^3}{\nu_m + j\omega}\right) dv. \tag{7.4}$$

The components $\underline{\underline{F}}_o^1$ and $\underline{\underline{F}}_1^1$ can be eliminated from Eq. 6.5 by substitution from Eqs. 6.6 and 6.7, and this yields the differential equation for F_o^o:

$$(\nu_x + \nu_i - q) F_o^o = (v^2/3\nu_m)\,\underline{\underline{\nabla}}_r^2 F_o^o + (1/v^2)\,\partial\left[(eu_c/3m)\,\nu_m v^2 (\partial F_o^o/\partial v + m\nu_m v^3 F_o^o/M\right]\Big/\partial v. \tag{7.5}$$

The energy, in electron volts, $u_c = eE_p^2/2m\left(\nu_m^2 + \omega^2\right)$, which is introduced here, turns out to be the average energy transferred from the field to an electron between collisions, and $\nu_m u_c$ is the power transfer. It is, in general, a function of the electron's energy through the collision frequency ν_m, and it is also a function of the external parameters E, p, and $\lambda = 2\pi c/\omega$. The power transfer has a maximum for $\nu_m = \omega$, and this corresponds to the pressure for optimum breakdown. At pressures above this value, u_c varies as $(E_p/p)^2$.

The total excitation and ionization rates may be defined by

$$n\bar{\nu}_x = \int_0^\infty \nu_x F_o^o\, 4\pi v^2 dv, \tag{7.6}$$

$$n\bar{\nu}_i = \int_0^\infty \nu_i F_o^o\, 4\pi v^2 dv, \tag{7.7}$$

and, since every exciting collision yields one, and every ionizing collision two, slow electrons, we have

$$\int_0^\infty qF_o^o\, 4\pi v^2 dv = n(\bar{\nu}_x + 2\bar{\nu}_i). \tag{7.8}$$

Use is made of these relations in multiplying Eq. 7.5 by $4\pi v^2 dv$ and integrating over all velocities. The term in brackets vanishes at both limits, and one obtains

$$n\bar{\nu}_i + \nabla_r^2 Dn = 0. \tag{7.9}$$

This is a diffusion equation and expresses the fact that at breakdown the ionization rate equals the diffusion rate. For a uniform electric field (which will be the assumption from here on), it has a solution which is everywhere positive only if $\bar{\nu}_i = D/\Lambda^2$, where Λ is a diffusion length. This may be called the breakdown condition.

8. Distribution in Energy

If the function F_o^o is assumed to be the product of a function n(x) of space and a function f(u) of the energy u, defined by $u = mv^2/2e$, we can make use of Eq. 7.9 to replace $\nabla_r^2 F_o^o$ by $-nf/\Lambda^2$ and obtain the following equation for f(u):

$$\left(\nu_x + \nu_i - q + \frac{2eu}{3m\,\nu_m \Lambda^2}\right) f = \frac{2}{3\sqrt{u}} \frac{d}{du} \nu_m u^{3/2} \left(u_c \frac{df}{du} + \frac{3m}{M} f\right). \tag{8.1}$$

The terms on the left side represent the electrons leaving unit volume of phase space through excitation, ionization, and diffusion, and their reappearance at low energy at the rate qf. On the right are the terms attributable to energy gained from the field and lost to recoil.

The excitation frequency ν_x sets in discontinuously at a potential u_x so that it is always necessary to divide the energy range into two parts and solve Eq. 8.1 for two functions, f_e and f_{xi}, appropriate to the elastic and inelastic ranges and join them at u_x. On the other hand, since $(\nu_x + \nu_i)$ may generally be approximated by a continuous function, it is not necessary to join functions at u_i. The method of solution appropriate to the two ranges is quite different, so that they must be discussed separately.

9. Inelastic Range

When inelastic collisions are possible, they dominate all other collision processes because of the large energy losses involved. Accordingly, the recoil and diffusion terms may be left out of Eq. 8.1. We may also neglect q in this range. The equation to be solved is then

$$2(d/du)\left(\nu_m u_c u^{3/2} df_{xi}/du\right) = 3(\nu_x + \nu_i) u^{1/2} f_{xi}. \tag{9.1}$$

The conditions imposed on the solution are somewhat contradictory; we must choose that solution that vanishes at infinity, but we want greatest accuracy just above u_x, where most of the excitations take place. The conventional asymptotic expansion does not satisfy the second requirement without an unreasonable number of terms, and the WKB

method diverges at u_x, but we can use a somewhat similar approximation.[1] Setting

$$u^{1/2} f_{xi} = e^{-s}, \tag{9.2}$$

the equation for s is

$$s'^2 - s'' - s'/2u - (s' + 1/2u)(d/du) \ln(\nu_m u_c) = 3(\nu_x + \nu_i)/2\nu_m u_c u. \tag{9.3}$$

An analytic approximation to the experimental data must now be substituted for $\nu_m u_c$ and $\nu_x + \nu_i$, and a power series in 1/u is substituted for s', the last term in the series being reserved to obtain exact agreement at u_x.

Knowing s, the average ionization frequency per electron is given by

$$\bar{\nu}_i = 2\pi(2e/m)^{3/2} \int_{u_i}^{\infty} \nu_i u^{1/2} f_{xi} du, \tag{9.4}$$

and the total inelastic frequency is given (see Eq. 10.1) by

$$(\bar{\nu}_x + \bar{\nu}_i) = -(4\pi/3)(2e/m)^{3/2} \left(\nu_m u_c u^{3/2} df_{xi}/du\right)_x . \tag{9.5}$$

The subscript indicates that the quantity in the parenthesis is to be taken at u_x. Both of these expressions contain an unknown normalization constant and so cannot be evaluated as they stand, but their ratio,

$$N_{xi} = 1 + \frac{\bar{\nu}_x}{\bar{\nu}_i} = -\frac{2}{3} \left(\nu_m u_c u^{3/2} \frac{df_{xi}}{du}\right)_x \Big/ \int_{u_i}^{\infty} \nu_i u^{1/2} f_{xi} du, \tag{9.6}$$

can be evaluated and has a physical meaning. Because one electron must leave the tube for every one produced, $1/\bar{\nu}_i$ is the average lifetime of a free electron from its liberation at an ionization to its absorption at the walls; $\bar{\nu}_x/\bar{\nu}_i$ is the average number of excitations produced by an electron during its lifetime; and the number N_{xi} represents the total inelastic collisions during an electron's free lifetime.

Because of the exponential nature of f_{xi}, the number N_{xi} depends primarily on $\exp(s_x - s_i)$. From Eq. 9.3 it is seen that the main part of s' is given by $\left[3(\nu_x + \nu_i)/2\nu_m u_c u\right]^{1/2}$ which, when $\nu_m > \omega$, is proportional to p/E_p. Accordingly, the variation of N_{xi} with p/E_p is given very nearly by

$$N_{xi} = \alpha \exp(\beta p/E_p), \tag{9.7}$$

where α and β are constants obtainable from Eq. 9.3.

---

1. For an equivalent approximation see Allis, Eq. 33.5.

10. Elastic Range

Below u_x, the excitation and ionization frequencies are zero, but we must discuss the appearance rate qF_o^o. In order to calculate it as a function of energy it is necessary to take the product of the distribution function and the excitation function of each level and shift the product down the energy scale by the energy of the particular level. Since the excitation functions of allowed transitions have a sharp maximum just above the excitation potential, the scattered electrons have very little energy. The excitation functions of forbidden transitions have a maximum far above the excitation potential, but there are a negligible number of electrons with sufficient energy to excite these. Accordingly, most inelastically scattered electrons have very little energy, and no appreciable error is made in assuming that q is a delta-function at zero energy.

Multiplying Eq. 8.1 by $4\pi v^2 dv$ gives the net rate of loss of electrons from the spherical shell of thickness dv. Integrating and making use of Eq. 7.8 gives

$$\bar{\nu}_x + 2\bar{\nu}_i - \frac{4\pi}{3\Lambda^2}\int_0^v \frac{f_e}{\nu_m} v^4 dv = -\frac{4\pi}{3}\nu_m v^3\left(u_c\frac{df_e}{du} + \frac{3m}{M}f_e\right), \tag{10.1}$$

where $\bar{\nu}_x + 2\bar{\nu}_i$ is the rate of appearance of electrons at small velocities. The integral represents losses by diffusion of electrons of speeds between zero and v, and its value at infinity would, by Eq. 7.9, equal $\bar{\nu}_i$. The difference represents the rate at which electrons pass the energy u in the upward direction in order to supply the inelastic processes occurring at higher energies. Equation 10.1 was derived by Smit[1] directly from this principle of balance between electrons going up in energy and the rate of inelastic collisions; however, Smit includes the thermal energy of the gas but does not include diffusion. In glow discharges the diffusion term is much larger than the thermal one. At very low pressures the diffusion term is quite large, and one must solve the second-order equation (8.1) for f_e; but in most cases the diffusion term is small and there is then a great advantage in replacing the integral by an approximation such as

$$\frac{4\pi}{3\Lambda^2}\int_0^v \frac{f_e v^4}{\nu_m} dv = \frac{\bar{\nu}_i \nu_m v^3}{\left(\nu_m v^3\right)_o} . \tag{10.2}$$

This expression gives the full diffusion loss $\bar{\nu}_i$ at the velocity v_o, which corresponds to the energy u_o (to be defined shortly), and the third power of the velocity was actually found to be the best in the case for which extensive numerical calculations were made. With this substitution, Eq. 10.1 becomes a first-order inhomogeneous equation. If we define an energy variable w by $dw = 3mdu/Mu_c$, the solution of the homogeneous part[2] is

---

1. J. A. Smit, Physica 3, 543 (1936).

2. M. J. Druyvesteyn, F. M. Penning, Rev. Mod. Phys. 12, 87 (1940); H. Margenau, Phys. Rev. 69, 508 (1946).

$$f_M = Ae^{-w}. \tag{10.3}$$

The solution of the complete equation for f_e is

$$f_e = \frac{3}{4\pi}\left\{(\bar{\nu}_x + 2\bar{\nu}_i)e^{-w}\int_u^{u_o} e^w \frac{du}{\nu_m u_c v^3} - \bar{\nu}_i\left(\frac{M}{3m}\right)\left(\frac{e^{w_o - w} - 1}{(\nu_m v^3)_o}\right)\right\}, \tag{10.4}$$

which, at higher pressures, can be replaced by the simpler function

$$f_e = \frac{3}{4\pi}(\bar{\nu}_x + \bar{\nu}_i)e^{-w}\int_u^{u_o} e^w du/\nu_m u_c v^3. \tag{10.5}$$

The constant of integration in both of these expressions appears as an energy u_o at which the function f_e crosses the axis when extended beyond u_x. The meaning of this energy is seen by noting that f_e would be unchanged if the actual excitation and ionization functions ν_x and ν_i were replaced at u_o by delta-functions with the proper relative magnitudes so that all inelastic collisions would take place at exactly that energy. Thus u_o is the equivalent single excitation potential. By this equivalence the diffusion should also vanish above u_o and hence the integral (10.2) must equal $\bar{\nu}_i$ at $v = v_o$.

The potential u_o is determined by equating the logarithmic derivatives of f_e and f_{xi} at u_x. In general, the extrapolation $u_o - u_x$ is small, and when this is so a linear extrapolation formula may be used. The first-order derivative may be eliminated from Eq. 8.1 by the standard transformation

$$g = (\nu_m u_c)^{1/2} u^{3/4} e^{w/2} f. \tag{10.6}$$

Then $g'' = 0$ when $g = 0$. The function $g(u)$ has a point of inflection at u_o and may be extrapolated linearly back to u_x, giving

$$-\frac{1}{u_o - u_x} = \left(\frac{g'}{g}\right)_x = \frac{1}{2}\frac{d\ \ln(\nu_m u_c)}{du} + \frac{1}{4u_x} + \frac{3m}{2Mu_c} - s'_x, \tag{10.7}$$

the whole right-hand side being taken at u_x. When this extrapolation is valid, the effective excitation potential u_o may be calculated from the inelastic function f_{xi} alone.

11. Breakdown Equation

The diffusion coefficient D may be calculated by substituting f_e and f_{xi} in Eq. 7.3. A negligible error is made by integrating f_e from 0 to u_o and not using f_{xi}, the difference being readily computed and shown to be small. Using Eq. 10.4 we get

$$D = \frac{2\pi}{3}\left(\frac{2e}{m}\right)^{5/2}\int_0^{u_o} f_e u^{3/2}\frac{du}{\nu_m} = \frac{u_o^2}{E^2}\left[(\bar{\nu}_x + \bar{\nu}_i)\mathscr{D} + \bar{\nu}_i\delta\right], \tag{11.1}$$

where $\mathscr{D}$ and δ are two dimensionless functions of v_o, and E is the rms value of the electric field:

$$\mathscr{D} = \frac{4}{v_o^4}\int_0^{v_o} \frac{v^4 e^{-w}}{\nu_m}\,dv \int_v^{v_o} \frac{\nu_m^2 + \omega^2}{\nu_m v^2}\, e^w dv, \tag{11.2}$$

$$\delta = \mathscr{D} - \frac{ME^2}{3mu_o^2(\nu_m v^3)_o}\int_0^{v_o} \frac{v^4}{\nu_m}\left[e^{w_o - w} - 1\right]dv. \tag{11.3}$$

The breakdown condition is then

$$\Lambda^2 E^2/u_o^2 = N_{xi}\,\mathscr{D} + \delta, \tag{11.4}$$

where Eq. 9.6 or Eq. 9.7 can be substituted for the inelastic collision number.

This general outline for a theory of ac breakdown has been made specific by a number of workers. For any particular gas, specific assumptions are made to render the problem mathematically tractable. These assumptions will now be discussed briefly.

12. Hydrogen

For hydrogen gas[1] the collision frequency ν_m is nearly independent of energy and is given by $\nu_m = 5.9 \times 10^9 p$ at all energies above 4 volts. The effective field E_e, defined by Eq. 1.5, is a constant, and in terms of this the average energy gain per collision is $u_c = 5 \times 10^{-5}(E_e/p)^2$ electron-volts.

When ν_m is constant the variable $2w/3$ is the ratio of recoil loss to energy gain per collision, the loss exceeding the gain if w is greater than 3/2. At the higher pressures breakdown is observed for w_i approximately 4, so that in these cases the electrons are losing more energy to recoil, in the average, than they gain from the field, over most of the energy range. There is a sufficient number of statistically lucky electrons, however, to overcome this handicap and reach the ionization potential, producing breakdown.

The integrals in Eqs. 11.2 and 11.3 can be evaluated in terms of incomplete gamma-functions or, more conveniently, by the series

$$\mathscr{D} = \frac{\nu_m^2 + \omega^2}{\nu_m^2} w_o^{-2}\int_0^{w_o} w^{3/2} e^{-w}\int_w^{w_o} t^{-3/2} e^t\,dt\,dw$$

$$= \frac{\nu_m^2 + \omega^2}{\nu_m^2}\, 4!\sum_0^{\infty} \frac{(k+1)!}{(2k+5)!}(4w_o)^k, \tag{12.1}$$

$$\delta = 3\,\frac{\nu_m^2 + \omega^2}{\nu_m^2}\, 4!\sum_0^{\infty} \frac{(k+1)!}{(2k+5)!}\,\frac{(4w_o)^k}{2k+7}\,.$$

1. W. P. Allis, S. C. Brown, Phys. Rev. 87, 419 (1952).

Ramien[1] has measured the excitation and ionization probabilities in hydrogen, and his data can be represented by the functions

$$(\nu_x + \nu_i)/\nu_m = h_o u - h_1 - h_2/u, \tag{12.2}$$

$$\nu_i/\nu_m = h_i(u - u_i), \tag{12.3}$$

with the constants $u_i = 16.2$ volts, $h_i = 9.2 \times 10^{-3}$ volt^{-1}, $u_x = 8.9$ volts. The values $h_o = 8.7 \times 10^{-3}$ volt^{-1} and $h_1 = 76 \times 10^{-3}$ are in agreement with his data. Agreement with the breakdown data could not, however, be obtained if the losses observed by Ramien below 8.9 volts and ascribed to the excitation of vibrations were included in the theory.

With the above inelastic collision functions we set

$$s = au - b \ln u + c/u. \tag{12.4}$$

The coefficients a and b are determined in the usual way for series near infinity,

$$a^2 = 3h_o/2u_c, \quad b = 3h_1/4au_c - \tfrac{1}{4}. \tag{12.5}$$

The coefficient c is used to obtain exact agreement at u_x. This gives

$$c/u_x = au_x - b + \tfrac{3}{4} - \left(2au_x - b + \tfrac{9}{16}\right)^{1/2}. \tag{12.6}$$

The approximation is then tested by substituting Eq. 12.4 with these constants in Eq. 9.1 and solving for $(\nu_i + \nu_x)$. This gives the theoretical excitation frequency for which Eqs. 9.2 and 12.4 are the exact solution, and it must agree closely with the experimental data for P_x and P_i, particularly between u_x and u_i. Substitution of Eqs. 9.2 and 12.4 in Eq. 9.6 gives the number of inelastic collisions per electron:

$$N_{xi} = \frac{h_o}{h_i} \frac{au_x - b + \frac{1}{2} - c/u_x}{\mathcal{J}(u_i)} \left(\frac{u_x}{u_i}\right)^b \times \exp\left[(a - c/u_i u_x)(u_i - u_x)\right], \tag{12.7}$$

where

$$\mathcal{J}(u_i) = \sum_{k=0}^{\infty} \sum_{\ell=0}^{\infty} \frac{(k + \ell + 1)!}{k!(au_i)^k} \frac{(b-\ell)!}{(b - k - \ell)!} \frac{\left(c/au_i^2\right)}{\ell!}.$$

This function agrees very well with the approximation (9.7) with $\alpha = 2$, $\beta = 71.7$ volts/cm-mm of Hg, for almost the whole range of the measurements. The limit $N_{xi} = 2$ as p/E approaches zero comes from the near equality of h_i and h_o, so that at high energies there are about equal numbers of excitations and ionizations. Introducing Eq. 12.4 into Eq. 10.7 we find the effective excitation potential from

$$1/(u_o - u_x) = a - 3m/2Mu_c - \left(b + \tfrac{1}{4}\right)/u_x - c/u_x^2. \tag{12.8}$$

1. H. Ramien, Z. Physik 70, 353 (1931).

Expressions 12.1, 12.7, and 12.8 may then be introduced in Eq. 11.4 to obtain a direct comparison with the quantities measured at breakdown. The results are shown in Fig. 4. The agreement is good over a wide range of pressure for several different values of Λ and at two different frequencies.

The disagreement at low pressures results from neglecting the diffusion term in f_{xi} and to the approximations made in the formula for the effective excitation potential u_o; at these pressures the more exact confluent hypergeometric functions of Section 13 should be used.

13. Rigorous Theory for Constant Collision Frequency

The Boltzmann transport equation is usually developed in terms of the electron velocity. However, for a constant collision frequency it is convenient to introduce the dimensionless independent variable w of Eq. 10.3 in the final differential equation.

The differential equation (8.1) written for the variable $w = 3mu/Mu_c$ is

$$f'' + f'\left[1 + (3/2w)\right] + f\left[(A/w) - (u_E/\Lambda E_e)^2\right] = 0,$$
$$A = \frac{3}{2} - (M/2m)(\nu_x + \nu_i - q)/\nu_m \tag{13.1}$$

where $u_E = u_c(M/3m)$. This equation is of second order. It has a pole of first order at the origin, $w = 0$, and an essential singularity at infinity, $w = \infty$. Since Eq. 12.2 is not valid for $u < u_x$, we have to divide the energy scale at $w = w_x$ and to discuss separately the integration of Eq. 13.1 in the two regions.

In the elastic collision range, below w_x, Eq. 13.1 takes the form

$$f_e'' + f_e'\left[1 + (3/2w)\right] + f_e\left[(3/2w) - (u_E/\Lambda E_e)^2\right] = 0. \tag{13.2}$$

The solution in terms of confluent hypergeometric functions is

$$f_e(w) = \left\{\left[M_1(w) + C_e w^{1/2} M_2(w)\right] \times \exp\left[-(g+1)w/2\right]\right\} C_{eN}, \tag{13.3}$$

where

$$M_1(w) = M\left(\alpha:\tfrac{3}{2}:gw\right); \quad M_2(w) = M\left(\alpha - \tfrac{1}{2}; \tfrac{1}{2}; gw\right),$$
$$\alpha = \tfrac{3}{4}(g-1)/g; \qquad g^2 = 1 + 4(u_E/\Lambda E_e)^2,$$

and C_e and C_{eN} are integration constants.

In the range of inelastic collisions between the electrons and the gas molecules, when the electron energy lies above u_x, Eq. 13.1 may be written as

$$f''_{xi} + f'_{xi}\left[1 + (3/2w)\right] - f_{xi}G(w) = 0,$$

$$G(w) = \tfrac{1}{2}(g^2 - 1)^{1/2} + h_o\, u_c\, (M^2/6m^2) \tag{13.4}$$

$$-\left[\tfrac{3}{2} + Mh_1/2m\right](1/w) - (3h_2/2u_c)(1/w)^2.$$

There exists only one asymptotic solution for Eq. 13.4 which fulfills the boundary condition that the distribution function shall vanish at infinity. It is

$$f_{xi}(w) = C_{eN}C_i w^{\left(K-\frac{3}{4}\right)}\left[\exp(-a_1 w)\right] \times \left[1 + \sum_{n=1}^{\infty}\prod_{r=1}^{n} p^{(r)}/n\,!\,(a_o w)^n\right],$$

where

$$a_o = \left[g^2 + 6h_o\left(u_E^2/u_c\right)\right]^{1/2}; \quad a_1 = \tfrac{1}{2}(a_o + 1);$$

$$K = (M/2m)\, h_1/a_o, \quad p^{(r)} = \frac{1}{16} - 3h_2/2u_c - \left[K + \tfrac{1}{2} - r\right]^2; \tag{13.5}$$

$$\prod_{r=1}^{n} p^{(r)} = p^{(1)}\, p^{(2)} \ldots p^{(n)}.$$

The integration constants C_e and C_i can be calculated by joining f_e and f_{xi} in value and slope at $w = w_x$. As a result of these processes we find

$$C_e = -(w_x)^{1/2}(M_{1x}/M_{2x})(T_1/T_o),$$

$$C_i = \left(1/2T_o M_{2x} w_x^{K+1/4}\right)\exp\left[(a_o + g)\, w_x/2\right],$$

$$T_o = \sum\nolimits'_x + \sum\nolimits_x\left[\left(K - \tfrac{1}{4}\right)/w_x - (a_o - g)/2 - gM'_{2x}/M_{2x}\right],$$

$$T_i = T_o + \sum\nolimits_x\left[g(M'_{2x}/M_{2x} - M'_{1x}/M_{1x}) - 1/2w_x\right], \tag{13.6}$$

$$\sum\nolimits_x = \sum_{r=0}^{\infty} P_r; \quad P_o = 1; \quad P_r = P_{r-1}\left(p^{(r)}/ra_o w_x\right),$$

$$\sum\nolimits'_x = -(1/w_x)\sum_{r=0}^{\infty} rP_r; \quad M_{1x} = M_1(w_x); \quad M_{2x} = M_2(w_x),$$

$$gM'_1 = \partial M_1(w)/\partial w; \quad gM'_2 = \partial M_2(w)/\partial w.$$

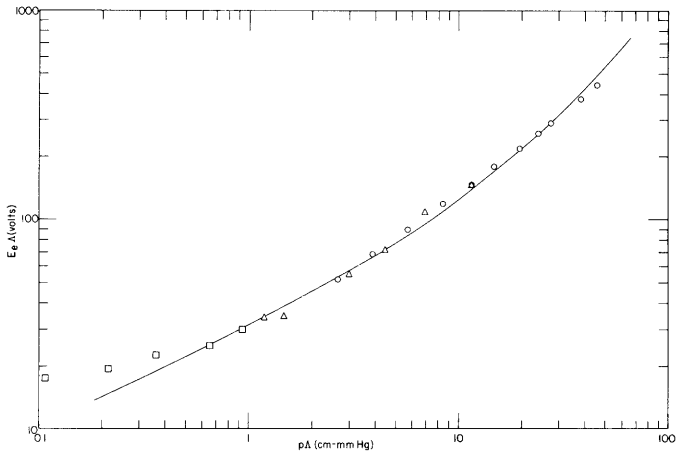

Fig. 4. Breakdown voltages as a function of pΛ for hydrogen. The line is theoretical; the points, experimental. ⊡ λ = 10.6 cm, Λ = 0.05 cm; ⊙ λ = 300 cm, Λ = 0.2 cm; △ λ = 10.6 cm, Λ = 0.028 cm

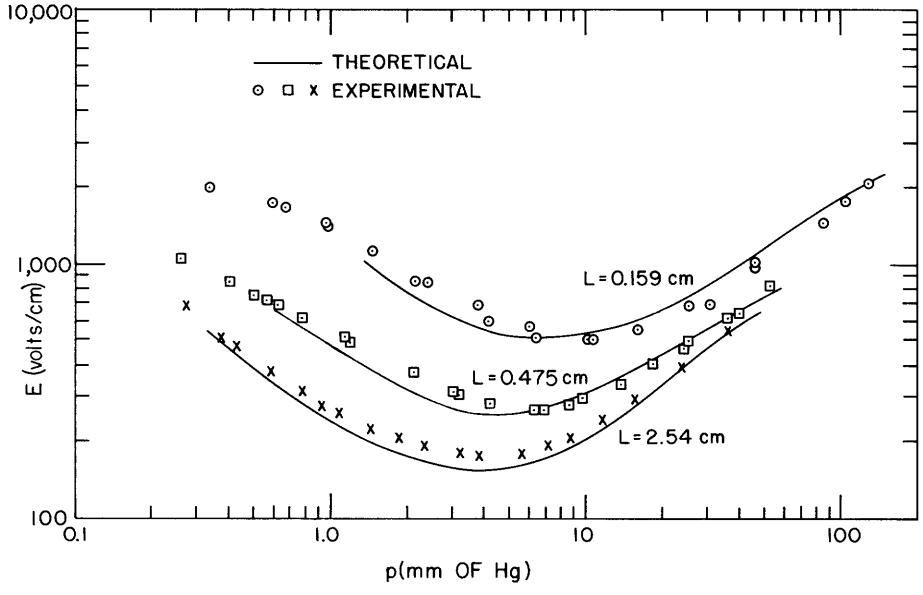

Fig. 5. Comparison of experimental and theoretical curves for breakdown in hydrogen at 3000 Mc/sec. The line is theoretical; the points are experimental

The breakdown condition can be written, $D = \Lambda^2 \bar{\nu}_i$, where both the diffusion coefficient and the ionization frequency terms depend on the distribution function. They are calculated from

$$D = \int_0^\infty (2e/3m\nu_m)\, u f^*(u)du,$$

$$\bar{\nu}_i = h_i \int_{u_1}^\infty \nu_m (u - u_i) f^*(u)du \tag{13.7}$$

where $f^*(u)du = 4\pi v^2 f(w)dv$, this function being the fraction of electrons within the energy limits $u \pm \frac{1}{2} du$. In the elastic range, the diffusion integral can be represented by confluent hypergeometric functions. In the inelastic range, we approximate the functions by Taylor series around w_i and w_x.

Inserting D and $\bar{\nu}_i$ in the breakdown equation yields a transcendental equation for $E_e\Lambda$ and E_e/p which may be evaluated in the form

$$\frac{(M/m)(h_i/u_i)(C_i/C_e)(u_E/a_1)^2 w_1^{k+3/4} \sum_i \exp(-a_1 w_1)}{1 + \left(2w_x^{\frac{3}{2}} \Big/ C_e C_{eN}\right)(f_{ex} + \partial f_{ex}/\partial w)} \times (1-\psi) = 1,$$

$$\psi = (2m/M)(u_i/h_i)\left[a_i/(\Lambda E_e)^2\right](u_x/u_i)^{k+3/4} \times \left(\sum\nolimits_D \Big/ \sum\nolimits_i\right) \exp\left[a_1 (w_i - w_x)\right],$$

$$\sum\nolimits_i = \sum_{n,\, r=0}^{\infty} B_n^{(r)}; \quad B_n^{(o)} = (u_x/u_i)^n P_n; \tag{13.8}$$

$$B_n^{(r)} = B_n^{(r-1)}\left[(r+1)/r\right]\left[\left(k + \tfrac{3}{4} - n - r\right)/(a_1 w_i)\right],$$

$$\sum\nolimits_D = \sum_{n,\, r=0}^{\infty} A_n^{(r)}; \quad A_n^{(o)} = P_n;$$

$$A_n^{(r)} = A_n^{(r-1)}\left[(k + (7/4) - n - r)/(a_1 w_x)\right].$$

The quantity ψ may be neglected for $E_e/p < 10$ v/cm mm Hg. The first equation of (13.8) represents the ratio of the net number of electrons produced in the region $u > u_x$ by ionization and diffusion to the number of electrons lost in the elastic collision range $u < u_x$ by diffusion. This ratio must be equal to unity in a steady state.

The rigorous treatment for constant collision frequency has been applied to

hydrogen[1] and helium.[2] For hydrogen, use of the numerical values given under Eqs. 12.2 and 12.3 yielded the agreement shown in Fig. 5. For helium[3], $h_o = 0.0175$ volt^{-1}, $h_1 = 0.665$, and $h_2 = -6.6$ volts in Eq. 12.2; and $h_i = 5.48 \times 10^{-3}$ volt^{-1}, with $u_i = 24.5$ volts, in Eq. 12.3. The excitation potential u_x was taken as 19.9 volts to allow a simple step approximation for the initial part of the excitation function. These values lead to the theoretical line, which is compared with experiment, in Fig. 6.

14. Impure Helium

Considerable simplification of the theory presented here results if no excitation need be considered. Such a case is realizable if small amounts of mercury vapor are added to helium, the gas we named Heg in Section 3. This synthetic gas adds the simplification of no excitation to the simplification of a constant collision frequency, and one may use it to test the validity of some of the mathematical assumptions necessary in obtaining the solutions previously discussed. The magnitudes of two effects have been thus tested: (a) the result of the overshoot in energy due to the fact that the most probable energy at excitation is higher than the excitation energy; and (b) the magnitude of the error introduced by the assumption of constant ν_m, where even for helium this is not true at low energies. For the mathematical details involved see a paper by MacDonald and Brown;[4] the magnitudes of these effects are illustrated in Fig. 7. The excellence of the agreement between the theory and experiment for this simple case is demonstrated in Fig. 8. It should be emphasized that although various experimental conditions have been set up to render mathematical manipulation easy, no adjustable parameters appear in the theory.

15. Neon

The high-frequency gas-discharge breakdown in neon has also been studied in detail.[5] In this gas, instead of the collision frequency being considered constant, a constant mean free path is the approximate assumption. The constant mean free path case is considerably more complicated than those previously described, and the distribution functions were calculated separately for the regions of low $p\lambda$ and high $p\lambda$, corresponding to $(v/\ell)^2 \ll \omega$ and $(v/\ell)^2 \gg \omega$. The reader is referred to the original paper[5] for the derivations of the appropriate equations the results of which are as follows.

In the low $p\lambda$ region, the breakdown condition gives an equation for calculating the breakdown electric field in the form

---

1. A. D. MacDonald and S. C. Brown, Phys. Rev. 76, 1634 (1949).
2. F. H. Reder and S. C. Brown, Phys. Rev. 95, 885 (1954).
3. H. Maier-Liebnitz, Z. Physik 95, 499 (1935).
4. A. D. MacDonald and S. C. Brown, Phys. Rev. 75, 411 (1949).
5. A. D. MacDonald and D. D. Betts, Canadian J. Phys. 30, 565 (1952); 32, 812 (1954).

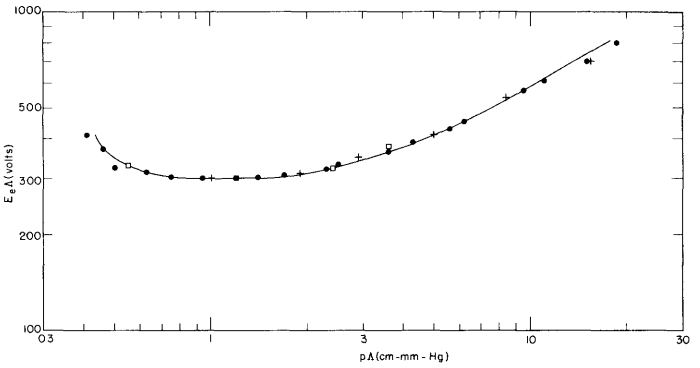

Fig. 6. High-frequency gas-discharge breakdown in pure helium

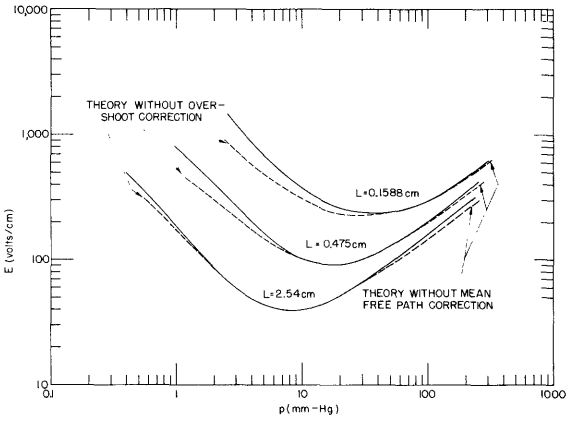

Fig. 7. Theoretical E-p curves illustrating the effect of various correction factors

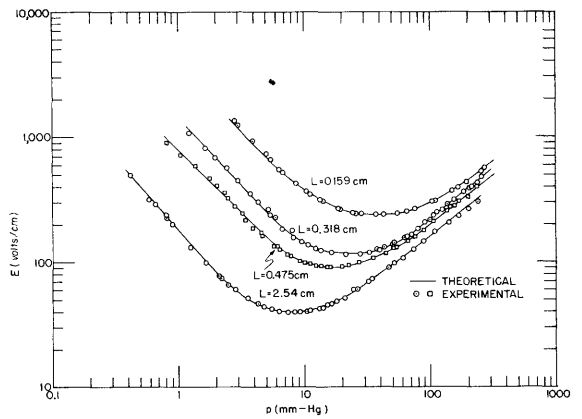

Fig. 8. Experimental breakdown electric fields compared with those theoretically predicted for Heg gas

$$\frac{1}{\Lambda^2} = \frac{3s^2}{r^3 \ell^2} \frac{Ah_{io}\left[e^{-y_i}(1+D) + D_{yi}E_i(-y_i)\right]}{\left\{2x_x\left[CI_o(x) - K_o(x)\right] - 4(x_x)^{1/2}Z_1(x_x) + 4 + A(s^2/r^2)\left[e^{-y_x} - DE_i(-y_x)\right]\right\}}. \tag{15.1}$$

Here, h_i is the ionization efficiency fitted to Maier-Liebnitz's data[1] as

$$\frac{\nu_i}{\nu_m} = h_i(u - u_o) = 4.48 \times 10^{-3}(u - 21.5).$$

The mean free path assumption is written as

$$\ell = 1/10p;$$

the other quantities are defined as follows:

$$x = us = u\left(1 - \frac{(p\Lambda)^2}{30.8}\right)\left(\frac{636}{E\Lambda p\lambda}\right)^2,$$

$$y = ur = u\left(\frac{412}{E\lambda}\right),$$

$$D = -\frac{\beta y_i^2}{(3+\beta)y_i + 4}; \quad \beta = \frac{412}{E\lambda}\left[16 - \frac{0.595}{(p\Lambda)^2}\right].$$

$Z_1(x) = K_1(x)^{1/2} + CI_1(x)^{1/2}$, where K_1 and I_1 are first-order Bessel functions of imaginary argument.

$$C = \frac{K_2(x)^{1/2} - \phi K_1(x)^{1/2}}{I_2(x)^{1/2} + \phi I_1(x)^{1/2}},$$

$$A = \frac{K_1(x)^{1/2} + CI_1(x)^{1/2}}{(x)^{1/2}e^{-y}(1/y + D/y^2)},$$

$$\phi = \frac{2r(x)^{1/2}}{s}\frac{\left[y^2 + (1+D)y + 2D\right]}{D_y + y^2},$$

and $E_i(-y_i)$ is the exponential integral

$$\int_{y_i}^{\infty} e^{-t}/t\, dt,$$

1. H. Maier-Liebnitz, Z. Physik 95, 499 (1935).

tables of which are available in Jahnke and Emde.[1] The subscripts i and x refer to ionization and excitation.

In the high pλ region, the breakdown is predicted by

$$\frac{1}{\Lambda^2} = \frac{6B}{a^2 \mu \ell^2} h_i \frac{e^{-az_i}}{\left\{ z_x e^{-z_x} \left[M_z(z_x) + F W_2(z_x) \right] - F/\delta + (B/a) e^{-az_x} \right\}} \tag{15.2}$$

$$h_i = 0.90 \times 10^{-4}; \qquad \mu = 1.62 \left(\frac{p}{10E} \right)^2,$$

$$z = u^2 \left(\frac{p}{E} \right)^2 / 123.4; \qquad \delta = \frac{30.8}{(p\Lambda)^2},$$

$$\rho = 4.2 \left(\frac{p}{10E} \right)^2; \qquad a = \frac{1}{2} \left(1 + \sqrt{1 + 4\rho/\mu^2} \right),$$

$$F = - \frac{\frac{d}{dz} M_1(z) + (a-1) M_1(z)}{\frac{d}{dz} W_1(z) + (a-1) W_1(z)},$$

$$B = e^{(a-1)z} \left[M_1(z) + F W_1(z) \right],$$

where the notation $M_1(z)$ holds for the confluent hypergeometric function $M(\delta; 1; z)$, with a similar notation for the second solution.

Equations 15.1 and 15.2 are implicit expressions for the breakdown electric field as a function of pressure, container size, and frequency of applied field. The breakdown fields are computed in practice by successive approximations. Breakdown curves for neon, both experimental and theoretical, are shown in Fig. 9.

b. The Effects of Nonuniform Fields

16. Cylinders of Arbitrary Length[2]

The differential equation and boundary condition that lead to the breakdown field strength are obtained from the continuity requirement on the electrons. The equation resulting from Eqs. 2.2 and 7.9 is

$$\nabla^2 \psi + \zeta E^2 \psi = 0, \tag{16.1}$$

where the electron diffusion current density potential ψ is given by $\psi = Dn$, and ζ is the high-frequency ionization coefficient. The boundary condition that ψ be zero on the walls of the discharge cavity is sufficiently accurate. The electric field appears

1. E. Jahnke and F. Emde, "Functionentafeln," Leipzig (1933).
2. M. A. Herlin and S. C. Brown, Phys. Rev. 74, 1650 (1948).

explicitly in Eq. 16.1 because it varies with position in the cavity. On the other hand, $p\lambda$ is constant throughout the cavity. The electric field in an arbitrary cavity is given in the form $E = E_o f(x, y, z)$, where E_o is the maximum value of the electric field, and f is a geometrical factor obtained from a solution for the field distribution within the cavity as an electromagnetic boundary value problem. The value of f is unity at the maximum field point. The degree of excitation of the cavity is expressed by E_o, and the relative field distribution through the cavity is independent of the excitation. The boundary value problem of finding a nonzero solution to Eq. 16.1, with the boundary condition that ψ be zero on the cavity walls, leads to a characteristic value of E_o, which is the breakdown field at the maximum field point.

Integration of Eq. 16.1 is simplified by the use of an approximation to the ionization coefficient. This approximation expresses the ionization coefficient as the simple analytic function

$$\zeta = \zeta_o \left(\frac{E}{E_o}\right)^{\beta-2} = \left(\frac{k}{E_o}\right)^2 \left(\frac{E}{E_o}\right)^{\beta-2}, \tag{16.2}$$

where ζ_o is the value of the ionization coefficient at the maximum field point. The quantity k is introduced for mathematical convenience in the following equations. It has the dimensions of reciprocal length, and appears multiplied into the radius variable below. The quantity $(\beta-2)$ is obtained as the slope of the ζ versus E/p plot on a logarithmic scale at the point E_o/p. This approximation gives accurate results because it is correct where the ionization is high, is inaccurate only where the ionization is low, and therefore has little effect on the solution of the equation.

The electric field in the TM_{010}-mode cylindrical cavity is given by the expression

$$E = E_o J_o(2.405r/R). \tag{16.3}$$

It depends on the radial coordinate only, which allows the differential equation, Eq. 16.1, to separate. Separation results in $\psi = A \sin(\pi z/L)\phi(r)$, where A is a constant, L is the length of the cylindrical cavity, z is the axial coordinate, and ϕ is a function only of r, determined from the differential equation

$$\frac{1}{r}\frac{d}{dr}\left(r\frac{d\phi}{dr}\right) + \left[\zeta E^2 - (\pi^2)/(L^2)\right]\phi = 0. \tag{16.4}$$

The approximation of Eq. 16.2 and the electric field of Eq. 16.3 substituted in Eq. 16.4 lead to the equation

$$\frac{1}{r}\frac{d}{dr}\left(r\frac{d\phi}{dr}\right) + \left[k^2 J_o^{\beta}(2.405r/R) - (\pi^2)/(L^2)\right]\phi = 0. \tag{16.5}$$

It is difficult to find an analytic solution to this equation. A good approximation is obtained by expressing the Bessel function as the first two terms of its power series. This approximation is also accurate where the ionization is high and fails only where it

is low. Equation 16.5 then becomes

$$\frac{1}{r}\frac{d}{dr}\left(r\frac{d\phi}{dr}\right) + \left\{k^2\left[1 - (r^2)/(b^2)\right] - (\pi^2)/(L^2)\right\}\phi = 0, \tag{16.6}$$

where

$$b = 0.831R/(\beta)^{1/2} \tag{16.7}$$

is the radius at which the ionization goes to zero under the assumptions given above.

The ionization function in Eq. 16.6 is negative beyond r = b, which is not physically correct. Accordingly, the ionization is set equal to zero from r = b to r = R. Equation 16.6 is used in the range $0 \leq r \leq b$, and in the range $b \leq r \leq R$ the equation

$$\frac{1}{r}\frac{d}{dr}\left(r\frac{d\phi}{dr}\right) - \frac{\pi^2}{L^2}\phi = 0 \tag{16.8}$$

is applied. The ionization function employed here is compared with the actual ionization function in Fig. 10. They are identical near r = 0, where the ionization is high. The error in the approximation becomes positive as r increases; negative, as it approaches the radius b. Beyond r = b, the ionization drops rapidly to zero and is approximated by the value zero. The boundary conditions on ϕ are that it be zero at r = R and that its derivatives and value match at r = b.

The solution of Eq. 16.6 is

$$\phi = \exp\left(-\frac{\sigma x^2}{2}\right) M\left[(2\sigma - 1)/(4\sigma),\ 1, \sigma x^2\right], \tag{16.9}$$

where

$$\sigma = 1/kb\left(1 - \frac{\pi^2}{k^2L^2}\right),$$

$$x = \left[1 - (\pi^2)/(k^2L^2)\right]^{1/2} kr,$$

and M is the confluent hypergeometric function. The second solution is omitted because it has a singularity at the origin. The solution of Eq. 16.8 is

$$\phi = iH_o^{(1)}(i\pi r/L) - \kappa J_o(i\pi r/L), \tag{16.10}$$

where κ is a constant of integration. It is chosen to make ϕ equal to zero at the point r = R, and it is thus a function of the ratio R/L.

The Bessel function in Eq. 16.10 is an exponentially increasing function of r; the Hankel function is an exponentially decreasing function of r. Therefore, κ is zero when R/L is infinity. The exponential decrease in electron density in the region where the ionization rate is very small, and assumed to be zero, is a result of diffusion to the end plates of the cavity. If R/L is not infinite, the negative exponentially increasing Bessel function term provides the extra decrease in electron density which causes it to go to

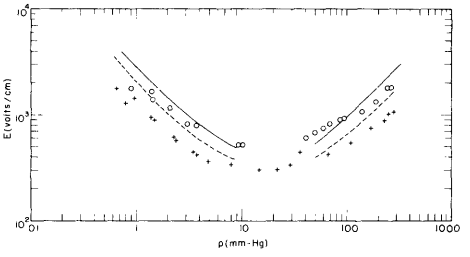

Fig. 9. Comparison of measured breakdown fields in neon with theory.
⊙ Λ = 0.101 cm
\+ Λ = 0.202 cm

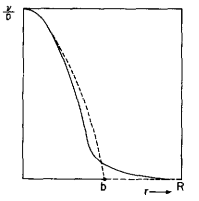

Fig. 10. Comparison of actual ionization function (solid curve) with its approximation (dotted curve)

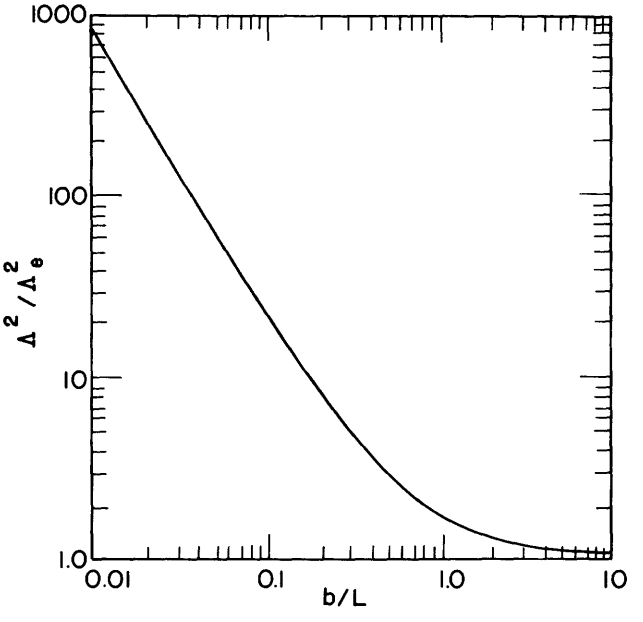

Fig. 11. The ratio of the effective diffusion length to real diffusion length for cylinders of arbitrary height as a function of the geometrical dimensions

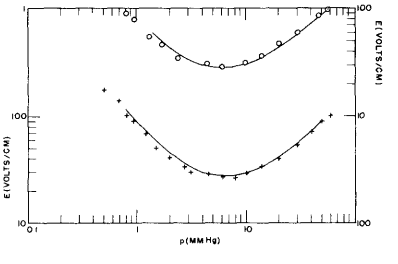

Fig. 12. Comparison of experimental points and theoretical curves for a cylindrical 3-inch cavity (+) and a spherical cavity (o) for Heg gas

zero at the finite cavity radius. Numerical computation of the relative magnitudes of these two terms shows, however, that for a wide range of the ratio R/L, the value of κ is very small and the contribution from the Bessel function term is correspondingly negligible. Thus, for R/L greater than 0.5, the Bessel term may be neglected. The range below 0.5 may be computed if the Bessel term is retained. The numerical computations were performed only for R/L > 0.5, so that the results presented here are applicable to cavities whose heights are smaller than their diameters. This increase in the coverage of the range of R/L is a substantial gain over the coverage of the parallel-plate treatment, for which R/L should be greater than 15.

The solutions given in Eqs. 16.9 and 16.10 should each be written with another constant of integration which appears as a multiplying constant. This constant is not written because the matching condition may be satisfied by making the ratio ϕ'/ϕ equal on both sides of the matching point r = b. The multiplying constant cancels in the ratio. The resulting equation is a transcendental equation for the breakdown field:

$$x_o \frac{H_1^{(1)}(ix_o)}{iH_o^{(1)}(ix_o)} = y_o \left[\frac{2\sigma - 1}{2\sigma} \frac{M\left(\frac{6\sigma - 1}{4\sigma}, 2, y_o\right)}{M\left(\frac{2\sigma - 1}{4\sigma}, 1, y_o\right)} - 1 \right], \tag{16.11}$$

where $x_o = \pi b/L$, and $y_o = kb$.

Equation 16.11 may be solved for kb as a function of kL. The results are most conveniently written by expressing $(\pi/kL)^2 = \Lambda_e^2$ as a function of b/L. This plot is shown in Fig. 11. Parallel-plate breakdown requires that $k = \pi/L$, so that the ordinate approaches unity for large b/L. If the tube is long or the slope of the ionization coefficient curve is large, b/L is small; and a larger value of k, and therefore electric field, is required for breakdown, relative to the value that would be required with a uniform field. The procedure used in finding E begins with a plot of ζ versus E/p. Assume a value of E_e/p, read β and ζ_e from the plot, and compute Λ_e. From this we determine $E_e = (\zeta_e)^{1/2}/\Lambda_e$ and compute the corresponding $p = E_e/(E_e/p)$. We can then determine E from E_e, p, and λ. Agreement between the calculated electric field in a TM_{010}-mode cavity and measured values for Heg gas is shown in Fig. 12.

17. Spherical Container[1]

The electric field in the lowest electric mode in a spherical cavity may be given by

$$E_r = E_o\left(\frac{a}{2.75r}\right) \cos\theta\, j_1(2.75r/a), \tag{17.1}$$

$$E_\theta = E_o\left(\frac{a}{2.75r}\right) \sin\theta \frac{d}{dr}\left[(2.75r/a) j_1(2.75r/a)\right], \tag{17.2}$$

$$E_\phi = 0,$$

1. A. D. MacDonald and S. C. Brown, Canadian J. Research 28, 168 (1950).

where r, θ, and ϕ are the spherical coordinates, a is the radius of the sphere, and j_1 is the first-order spherical Bessel function.

It is seen that the electric field depends on both r and θ the introduction of which makes Eq. 16.1 inseparable. However, in breakdown, we are interested only in the energy transfer from the field to the electrons so that we need take into account only the magnitude of the field at a given point. Near the center of the cavity, where the field, and therefore the ionization, is high, the magnitude of the electric field is approximately spherically symmetric. If we assume that the electric field may be expressed as the average of these values over the whole of the cavity, we may write

$$E = E_o\left[1 - (r/a)^2\right]. \tag{17.3}$$

This is a good approximation to the average electric field except near the boundaries, where it does not matter.

The assumption that the electric field is independent of θ and ϕ makes ψ independent of these variables. Therefore, with the assumption of Eq. 16.2, we may write Eq. 16.1 as

$$\frac{1}{r^2}\frac{d}{dr}\left(r^2\frac{d\psi}{dr}\right) + k^2\left(\frac{E}{E_o}\right)^\beta \psi = 0, \tag{17.4}$$

and introducing the value of E from Eq. 17.3, we have

$$\frac{1}{r^2}\frac{d}{dr}\left(r^2\frac{d\psi}{dr}\right) + k^2\left[1 - (r/a)^2\right]^\beta \psi = 0. \tag{17.5}$$

We expand the term in r/a by the binomial theorem and drop powers of (r/a) greater than 2. This makes an appreciable error only near the boundaries, where again the accuracy of the method is unimportant. Then

$$\frac{d^2\psi}{dr^2} + \frac{2}{r}\frac{d\psi}{dr} + k^2(1 - \mu^2 r^2)\psi = 0, \tag{17.6}$$

where $\mu^2 = \beta/a^2$; $1/\mu$ is the radius at which the ionization goes to zero under the assumptions given above. Beyond $1/\mu$ these assumptions lead to a negative ζ, which is not physically correct, so we set $\zeta = 0$ for $r > 1/\mu$.

For mathematical convenience, we transform to a dimensionless independent variable and let $k\mu r^2 = x$; the equation (17.6) becomes

$$\frac{d^2\psi}{dx^2} + \frac{3}{2x}\frac{d\psi}{dx} + \frac{k^2}{x}\left(\frac{1}{4k\mu} - \frac{x}{4k^2}\right)\psi = 0; \quad x < \frac{k}{\mu}. \tag{17.7}$$

We transform the dependent variable by letting

$$\psi = e^{-x/2}g,$$

and

$$\frac{d^2g}{dx^2} + \frac{dg}{dx}\left(\frac{3}{2x} - 1\right) - \frac{ag}{x} = 0, \tag{17.8}$$

where

$$a = \frac{3}{4} - \frac{k}{4\mu}.$$

Equation 17.8 is the equation for the confluent hypergeometric function in parameters 3/2 and a. The second solution is not allowed by the boundary condition, and therefore

$$\psi_1 = e^{-x/2} M\left(a; \frac{3}{2}; x\right), \tag{17.9}$$

where we designate by ψ_1 that part of ψ for which r is less than $1/\mu$, or x is less than k/μ. When x is less than k/μ, ζ is zero, and the differential equation (16.1) becomes

$$\frac{d}{dx}\left(x^{3/2}\frac{d\psi}{dx}\right) = 0,$$

of which the solution is

$$\psi_2 = C\left[1 - \left(\frac{x_o}{x}\right)^{1/2}\right], \tag{17.10}$$

where $x_o = k\mu a^2$ and is determined by the condition that ψ_2 shall be zero on the boundary; C is an arbitrary constant. We must match the solutions of Eqs. 17.9 and 17.10 at the point where $r = 1/\mu$, and therefore

$$\frac{\psi_1'}{\psi_1} = \frac{\psi_2'}{\psi_2},$$

which gives us

$$\frac{2/3\ aM(a+1;\ 5/2;\ x_1)}{M(a;\ 3/2;\ x_i)} - \frac{1}{2} = \frac{1}{2x_1\left[\left(\frac{x_1}{x_o}\right)^{1/2} - 1\right]}, \tag{17.11}$$

where

$$x_1 = k/\mu = \frac{ka}{\beta^{1/2}}.$$

Equation 17.11 relates a (the radius of the cavity), β (determined from the slope of the ζ curve), and k, which is inversely proportional to the characteristic diffusion length. The equation may be written in the form

$$\left[\frac{2/3\ aM(a+1;\ 5/2;\ y)}{M(a;\ 3/2;\ y)} - \frac{1}{2}\right] 2y = \frac{x}{1-x}, \tag{17.12}$$

where

$$\alpha = \frac{3 - y}{4}, \quad y = \frac{ka}{\beta^{1/2}}, \quad \text{and} \quad x = \beta^{1/2}.$$

Equation 17.12 is an equation in which the left side is a function of $ka/\beta^{1/2}$ only, and the right side is a function of $\beta^{1/2}$ only. Therefore it is a simple matter to find ka as a function of β. For the case of a uniform field, the characteristic diffusion length in a sphere is a/π, and inspection of Eq. 16.1 indicates that for a uniform field, $k = \pi/a$. We can now consider k as a measure of the effective radius of the discharge for diffusion; ka/π is then Λ/Λ_e, where Λ is the characteristic diffusion length as determined by the geometry of the container, and Λ_e is the effective characteristic diffusion length. Equation 17.12 is solved numerically and plotted in a fashion similar to that of Fig. 11.

In Fig. 12 are plotted the theoretical values of E as a function of p for a spherical cavity for Heg gas, using the calculated values of Λ_e. Agreement with experiment is also shown.

18. Coaxial Cylinders[1]

The value of ζE^2 as a function of position in the discharge cavity is obtained, and from the electric field as a function of position, we have

$$E = (V/r \ln b/a) \sin \pi z/L,$$

where V is the "voltage" at the center of the coaxial cavity, a and b are the inner and outer conductor radii, L is the length of the cavity, and r and z are the radial and axial space coordinates. This expression applies to a cavity a half-wavelength in length, which was used experimentally.

The expression given above for the electric field is a function of two space coordinates and leads to a nonseparable differential equation. This difficulty can be avoided by choosing an inner conductor radius which is small compared to the length L, which is a half-wavelength. Since the electric field in the region near the center conductor does not vary much with distance along the conductor, the conditions of infinite length are approached. We may consider the field to be given by the formula

$$E = V/r \ln(b/a), \tag{18.1}$$

from which ζE^2 is computed as a function of position. To this approximation Eq. 16.1 is a second-order linear differential equation in r only.

Equations 16.1, 18.1, and 16.2 now combine into

$$\frac{d^2\psi}{dr^2} + \frac{1}{r}\frac{d\psi}{dr} + k^2 \left(\frac{a}{r}\right)^{\beta} \psi = 0, \tag{18.2}$$

whose solution is

---

1. M. A. Herlin and S. C. Brown, Phys. Rev. 74, 910 (1948).

$$\psi = Z_o\left[\frac{2}{\beta - 2}\, ka\left(\frac{a}{r}\right)^{1/2(\beta-2)}\right], \tag{18.3}$$

where Z_o is a Bessel function of zero order. The boundary condition that $\psi = 0$ at $r = a$ and $r = b$ leads to the following transcendental equation expressing the breakdown condition

$$J_o(x)\, N_o\left[(b/a)^{1/2(\beta-2)}x\right] - J_o\left[(b/a)^{1/2(\beta-2)}x\right] N_o(x) = 0, \tag{18.4}$$

where

$$x = \frac{2}{\beta - 2}\, ka\left(\frac{a}{b}\right)^{1/2(\beta-2)}. \tag{18.5}$$

Roots of this equation are tabulated, giving x as a function of $(b/a)^{1/2(\beta-2)}$. Multiplying x by $(b/a)^{1/2(\beta-2)}$, gives $\left[2/(\beta-2)\right] ka$ as a function of $(b/a)^{1/2(\beta-2)}$.

The agreement between theory and experiment is illustrated in Fig. 13 for the breakdown between coaxial cylinders in air.

c. Effects of a Superimposed DC Field

19. Breakdown in Hydrogen

Solutions for the energy distribution function of electrons in a gas show a very close similarity between the distribution functions under the action of ac and of dc fields.[1,2] This similarity makes it possible to modify the ac distribution function theory for breakdown to take account of the superposition of a dc field and thus to predict the behavior of breakdown with both fields acting.

The gas in a cavity will break down when the losses of electrons to the walls of the cavity are replaced by ionization in the body of the gas. When an ac field alone is applied, electrons are lost by diffusion. When a small dc sweeping field is applied, electrons are lost both by diffusion and mobility. The breakdown condition can be formulated mathematically by a consideration of these processes.

The dc flow of electrons $\underline{\underline{\Gamma}}$ is given by

$$\underline{\underline{\Gamma}} = -n\mu \underline{\underline{E}}_{dc} - D\nabla n. \tag{19.1}$$

When the electrons that are lost are replaced by new ones resulting from ionization, we have

$$\nabla \cdot \underline{\underline{\Gamma}} = \nu_i n. \tag{19.2}$$

If the divergence of Eq. 19.1 is equated to $\nu_i n$, and $\underline{\underline{E}}_{dc}$ is directed along the z-axis, we obtain

1. T. Holstein, Phys. Rev. 69, 50 (1946).
2. L. J. Varnerin and S. C. Brown, Phys. Rev. 79, 946 (1950).

$$\nabla^2 n + \frac{E_{dc}}{D/u}\frac{\partial n}{\partial z} + \left(\frac{\nu_i}{D}\right) n = 0. \tag{19.3}$$

Equation 19.3 can be solved readily for a cylinder of axial height L and axial coordinate z, radius R, and radial coordinate r.

By separation of variables,

$$n = M(r)N(z),$$

we obtain two equations

$$\nabla_r^2 M + k_1^2 M = 0,$$

$$\frac{d^2N}{dz^2} + \frac{E_{dc}}{D/\mu}\frac{dN}{dz} + \left(\frac{\nu_i}{D} - k_1^2\right)N = 0, \tag{19.4}$$

where k_1^2 is the separation constant, and ∇_r^2 is the two-dimensional Laplacian in the plane perpendicular to z. The solutions are

$$M = \text{const. } J_o(k_1 r), \tag{19.5}$$

$$N = \text{const. } \sin(\pi/L)\, z \exp(-\mu E_{dc} z/2D), \tag{19.6}$$

where $k_1 = 2.404/R$, and J_o is the zero-order Bessel function. The exponential represents the deformation of the sine caused by the sweeping of electrons. This solution is subject to the condition

$$\nu_i/D = 1/\Lambda_{dc}^2, \tag{19.7}$$

where Λ_{dc} defines a modified diffusion length given by the relation

$$1/\Lambda_{dc}^2 = 1/\Lambda^2 + \left[E_{dc}/(2D/\mu)\right]^2. \tag{19.8}$$

For this case, the characteristic diffusion length is given by

$$1/\Lambda^2 = (\pi/L)^2 + (2.404/R)^2. \tag{19.9}$$

The only difference between the breakdown condition (19.7) in the ac-dc case and the pure ac case is the substitution of a modified diffusion length Λ_{dc} for the characteristic diffusion length Λ. Note that the modified diffusion length of a cavity is smaller than the characteristic diffusion length. A cavity whose electron losses are increased by a dc sweeping field is equivalent to a smaller cavity without a sweeping field.

Using the proper distribution function theory to calculate breakdown[1] and the modified diffusion length presented here, a theoretical breakdown curve for an $(E/p)_{dc}$ of 12 volts/cm has been obtained. The effect of superimposing a dc field on an ac field

1. L. J. Varnerin and S. C. Brown, Phys. Rev. 79, 946 (1950).

is illustrated in Fig. 14.

d. Effects of a Superimposed Magnetic Field

The breakdown of gases by high-frequency electric fields in the presence of a constant magnetic field has been studied by Townsend and Gill;[1] by A. E. Brown;[2] and by Lax, Allis, and S. C. Brown.[3] As in the case of strictly ac field breakdown, two approaches are available: the average electron theory and the distribution function theory. As there are advantages to each, both will be used. In Section 20, the average electron theory is given. In this method the orbit of a free electron in the assumed fields is computed first, and from this one computes the displacement and the energy gain in the time $\tau = t - t_o$ elapsed since a collision. These quantities are then averaged over the phase of the ac field at the time t_o of the last collision, over the direction in space of the velocity after the collision, and over the free time up to the next collision. The result is the mean-square displacement and energy gain of the average electron between collisions. One can then discuss an average electron from its initial low energy until it ionizes a gas atom or diffuses out of the tube. The condition for breakdown is that these two final achievements shall be equally probable. This method has the advantage that each step in the analysis has a direct physical meaning.

In Section 21 the Boltzmann transport equation is expanded in spherical harmonics in space and in Fourier series in time. There results a differential equation for the distribution function, which is integrated. Most of the properties of a discharge follow directly from a knowledge of the distribution function.

20. Average Electron Theory

Consider the motion of an electron between collisions under the influence of a uniform electric field along the x-axis, $E = E_p \exp(j\omega t)$, and a uniform and constant magnetic field B along the z-axis. The equation of motion is then

$$\underline{F} = -e\underline{E} - e\underline{v} \times \underline{B} = m\dot{\underline{v}}. \tag{20.1}$$

The solution of this equation is the sum of a general and a particular integral, which correspond to the superposition of a random circular helical motion and a plane elliptical motion. For the helical motion, whose axis is along the magnetic field, the velocity is

$$\begin{aligned} v_{1x} &= (a + jb) \exp(j\omega_b \tau) \\ v_{1y} &= (b - ja) \exp(j\omega_b \tau) \\ v_{1z} &= c \end{aligned} \tag{20.2}$$

---

1. J. S. Townsend and E. W. B. Gill, Phil. Mag. 26, 290 (1938).
2. A. E. Brown, Phil. Mag. 29, 302 (1940).
3. B. Lax, W. P. Allis, and S. C. Brown, J. Appl. Phys. 21, 1297 (1950).

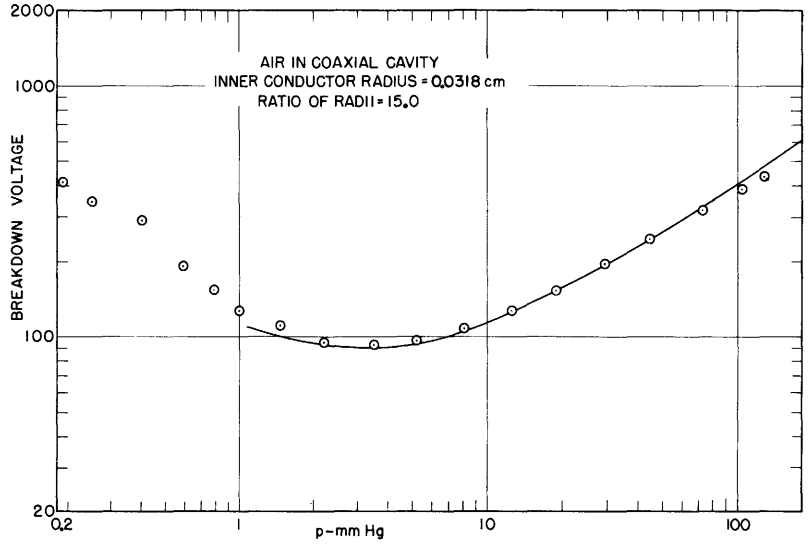

Fig. 13. Comparison of experimental points and theoretical curve for coaxial breakdown

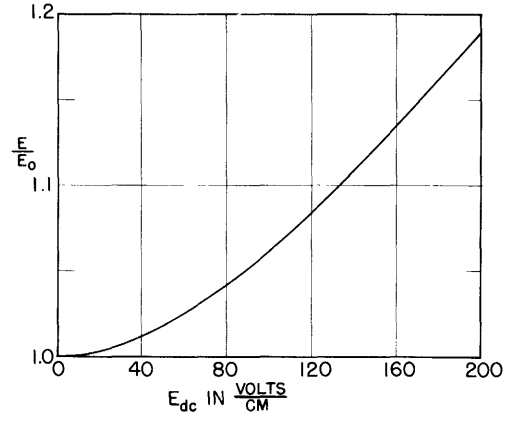

Fig. 14. Relative increase of ac breakdown field with superimposed dc field for air at a pressure of 38 mm Hg

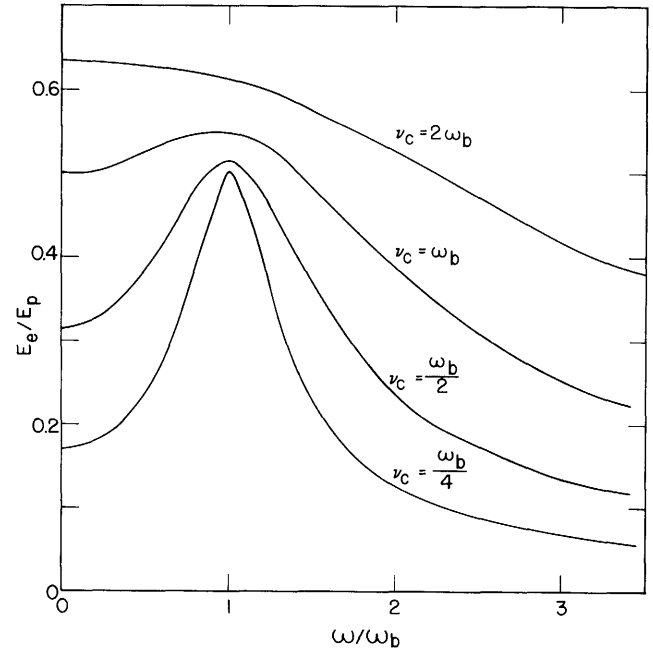

Fig. 15. Effective field as a function of the frequency, showing the resonance in the presence of a magnetic field

and oscillates at the cyclotron frequency $\omega_b = eB/m$. The helical motion contains the three arbitrary constants; the energy of this motion is constant and is given in electron-volts by

$$u_1 = \frac{mv_1^2}{2e} = \frac{m}{e}\,\frac{a^2 + b^2 + c^2}{2}. \tag{20.3}$$

For the elliptical motion, the velocity is

$$\begin{aligned} v_{2x} &= \frac{eE_p}{m}\,\frac{j\omega}{\omega^2 - \omega_b^2}\exp(j\omega t) \\ v_{2y} &= \frac{eE_p}{m}\,\frac{\omega_b}{\omega^2 - \omega_b^2}\exp(j\omega t) \end{aligned} \tag{20.4}$$

and oscillates at the frequency of the applied field.[1] The kinetic energy of this motion is uniquely determined by the magnitude and frequency of the applied field and is given by

$$u_2 = \frac{eE_p^2}{8m}\left[\frac{1}{(\omega - \omega_b)^2} + \frac{1}{(\omega + \omega_b)^2} + \frac{2\cos 2\omega t}{\omega_b^2 - \omega^2}\right]. \tag{20.5}$$

The total energy $u = (m/2e)(\underline{v}_1 + \underline{v}_2)^2$ will contain cross-product terms u_{12} which are important but rather lengthy to write down. Their value will be given later. The three constants, a, b, c, of the helical motion are determined by the velocity $\underline{v}_o = \underline{v}_1(\tau=0) + \underline{v}_2(t = t_o)$ immediately after a collision. Since the time τ has been used in Eq. 20.2, we have simply

$$\begin{aligned} a &= v_{ox} + \frac{eE_p}{m}\,\frac{\omega}{\omega^2 - \omega_b^2}\sin(j\omega t_o) \\ b &= v_{oy} - \frac{eE_p}{m}\,\frac{\omega_b}{\omega^2 - \omega_b^2}\cos(j\omega t_o) \\ c &= v_{oz}. \end{aligned} \tag{20.6}$$

It is noted that the elliptical motion exhibits a resonance at frequencies near the cyclotron frequency. Exactly at this frequency, Eqs. 20.4 no longer hold, and the solution corresponds to a spiral; as collisions interrupt the motion it will not be necessary to use this singular solution.

From the velocities one obtains the displacements x_1, y_1, z_1, x_2, y_2 by integration. From these the mean displacements $\langle x_1 \rangle$, etc., can be calculated, but these all

1. Allis, Eqs. 3.2 and 3.4.

vanish on averaging over orientations of v_o, which is assumed isotropic, and over collision times t_o. In the average, an electron stays where it is in a high-frequency discharge.

We are interested, however, in the mean-square displacements $\langle x_1^2 \rangle$, $\langle y_1^2 \rangle$, $\langle z_1^2 \rangle$ because these lead to the diffusion coefficient. One finds that the cross-product terms such as $\langle x_1 y_1 \rangle$ all vanish when averaged.

$$x_1^2 + y_1^2 = 2\,\frac{a^2 + b^2}{\omega_b^2}(1 - \cos\omega_b\tau)$$

$$z_1^2 = c^2\tau^2. \tag{20.7}$$

Averaging over orientations and times t_o, one finds that

$$\langle a^2 \rangle = \langle b^2 \rangle = \langle c^2 \rangle = \frac{v_1^2}{3}; \quad \langle ab \rangle = 0. \tag{20.8}$$

The cross terms between the helical and elliptical motions also vanish, but terms $\langle x_2^2 \rangle$ and $\langle y_2^2 \rangle$ do not vanish. However, these terms represent the mean-square displacements from mobility in the applied ac field and are not wanted in calculating the diffusion.

The average of a quantity X over the free times $\tau_m = 1/\nu_m$ between collisions is, by definition,

$$X = \int_0^\infty X \exp(-\nu_m\tau)\,\nu_m d\tau. \tag{20.9}$$

Applying this to the quantities in Eqs. 20.7 and defining the diffusion coefficients in terms of the mean-square displacements, we obtain[1]

$$D_{yy} = D_{xx} = \frac{\langle x_1^2 \rangle}{2\tau_m} = \frac{v_1^2 \nu_m}{3\left(\omega_b^2 + \nu_m^2\right)}$$

$$D_{zz} = v_1^2/3\nu_m. \tag{20.10}$$

This definition of the diffusion tensor is of necessity symmetric. We shall see later that there are skew-symmetric terms which the random-walk definition cannot give. Diffusion along the z-axis is not altered by the magnetic field, but in the plane at right angles to the field it is reduced in the ratio $\nu_m^2/\left(\omega_b^2 + \nu_m^2\right)$. For a given collision frequency, the diffusion coefficient is proportional to the energy of the electrons in their

1. Allis, Eq. 13.8.

helical motion.[1]

The mean energy gain between collisions is best obtained by considering the power input to an electron $P = -e\underline{\underline{E}} \cdot \underline{v}$. Since the velocity v_{2x} is out of phase with the field, the corresponding power P_2 into this motion is zero in the average, and only the power P_1 need be considered, where

$$P_1 = -eE_p \cos\omega t(a \cos\omega_b\tau - b \sin\omega_b\tau), \tag{20.11}$$

and the constants a and b are given by Eqs. 20.6. In averaging over orientations of the initial velocity the terms in v_o drop out. Averaging over t_o yields

$$\overline{P} = \frac{e^2E_p^2}{4m}\left[\frac{\sin(\omega + \omega_b)\tau}{\omega + \omega_b} + \frac{\sin(\omega - \omega_b)\tau}{\omega - \omega_b}\right] \tag{20.12}$$

from which the average energy is obtained by integrating with respect to τ from 0 to τ.

$$\langle u_{12}\rangle = \frac{eE_p^2}{4m}\left[\frac{1 - \cos(\omega + \omega_b)\tau}{(\omega + \omega_b)^2} + \frac{1 - \cos(\omega - \omega_b)\tau}{(\omega - \omega_b)^2}\right]. \tag{20.13}$$

Averaging this quantity over collision times gives the mean energy gain between collisions:

$$u_c = \frac{eE_p^2}{4m}\left[\frac{1}{(\omega + \omega_b)^2 + \nu_m^2} + \frac{1}{(\omega - \omega_b)^2 + \nu_m^2}\right] \equiv \frac{eE_e^2}{m\nu_m^2}. \tag{20.14}$$

This is a fundamental quantity in this theory. At low pressures ($\nu_m \to 0$) we see that it approaches twice the mean energy $\overline{u}_2$ of the elliptical motion of an electron, and in no case does it exceed this. At higher pressures, many collisions per oscillation, the energy u_2 loses its meaning, and the collision energy becomes $eE_p^2/2m\nu_m^2$. One can use Eq. 20.14 to define an effective field E_e which is the root-mean-square field at high pressure. This concept is useful when the collision frequency ν_m is independent of velocity because this single function takes into account the effects of frequency and magnetic field on the energy.

At low pressures the effective field has a maximum at resonance with the cyclotron frequency, as shown in Fig. 15.

The electrons produced by ionization have initially very little energy, but this increases by steps of u_c until the energy reaches a value u_i, at which ionization occurs. This is above the ionization potential V_i by an amount which we shall neglect. Excitations are disregarded in the following simple theory. The number N of free times for ionizing is $N = u_i/u_c$ when ν_m is constant.

The electrons thus double their number by ionization every N collisions, and unless

---

1. A more complete discussion of this is given in Allis, section 13.

some equally effective process exists which removes electrons their number will increase exponentially. In most cases, diffusion to the walls of the discharge tube is the balancing process. In absence of the magnetic field, the random-walk theory gives the mean-square distance $\Lambda^2 = N\ell^2/3$ reached in N free paths of mean-square length ℓ^2, so that if the average electron reaches the wall in a distance Λ the diffusion process will just balance ionization. This is the condition for breakdown, and we can write it

$$\frac{u_c}{u_i} = \frac{\langle \ell^2 \rangle}{3\Lambda^2} = \frac{\langle v^2 \rangle}{3\Lambda^2 \nu_m^2}, \tag{20.15}$$

where Λ is now a length characteristic of the discharge tube.

If there is a magnetic field, u_c will be altered according to Eq. 20.14. At the same time the random-walk theory must be altered to take into account the curved paths between collisions. This may be done by appropriately decreasing ℓ or increasing Λ. We shall adopt the latter procedure and denote the new length by Λ_e. Its value will be given later.

When the mean free path is much smaller than Λ_e, the intercollision energy gain u_c is correspondingly smaller than the ionization potential. From Eq. 20.15 we see that breakdown should occur at the same effective field if the ratio of the mean free path to the effective diffusion length is the same; that is, the effective field for breakdown is a function of $p\Lambda_e$ only.

Combining Eqs. 20.14 and 20.15 we get an expression similar to Eq. 3.3:

$$E_e^2 = \frac{2}{3}\frac{\bar{u}u_i}{\Lambda_e^2}. \tag{20.16}$$

Experimental data for breakdown in Heg are shown in Fig. 16. This resonance effect of the magnetic field and the high frequency are removed by using the effective field.

In order to test Eq. 20.10 for the diffusion coefficient, breakdown was studied in a flat cylindrical cavity whose length was very short compared to the radius. With the magnetic field placed transverse to the axis most of the diffusion has to take place perpendicular to the magnetic field and hence will show the full reduction. By Eq. 20.10, the mean square of the distance traveled by an electron is proportional to the diffusion coefficient D, and therefore the effective diffusion length Λ_e appropriate to infinite parallel plates is

$$\Lambda_e^2 = \frac{\omega_b^2 + \nu_c^2}{\nu_m^2}\Lambda^2. \tag{20.17}$$

The effect of a magnetic field is to make the dimensions of the cavity at right angles to the field appear larger to an electron. By Eq. 20.16 this should reduce the effective

field for breakdown in the same proportion.

However, Eq. 20.16 does not correspond with experiment except when used for comparative purposes. Equation 20.14 and the random-walk theory give the number of free times for the average electron to ionize and reach the wall, respectively. But in a discharge it is the faster-than-average electron that ionizes and the more-mobile-than-average electron that leaves the tube, and these are not the same electron. The mean free path method must therefore fail in predicting quantitative breakdown, and the failure should be worst when there are many collisions and therefore the greatest deviations from the mean.

21. Boltzmann Theory

Introducing the magnetic field into the Boltzmann transport equation, Eq. 6.1, gives

$$C = \frac{\partial F}{\partial t} + \nabla \cdot (\underline{\underline{v}} F) - \nabla_v \cdot \frac{e\underline{\underline{E}} F}{m} - \nabla_v \cdot \frac{e}{m} \underline{\underline{v}} \times \underline{\underline{B}} F. \tag{21.1}$$

Using Eq. 6.2, we obtain

$$(\nu_x + \nu_i - q) F_o^o + \frac{m}{M} \frac{1}{v^2} \frac{\partial}{\partial v} \left(\nu_m v^3 F_o^o\right) - \frac{v}{3} \nabla \cdot \underline{\underline{F}}_1^o + \frac{e}{m} \frac{1}{3v^2} \frac{\partial}{\partial v} \left[\frac{v^2}{2} \underline{\underline{E}}_p \cdot \left(\underline{\underline{F}}_1^1\right)_{real}\right] = 0$$

$$\nu_m \underline{\underline{F}}_1^o + v \nabla F_o^o - \frac{e}{m} \underline{\underline{B}} \times \underline{\underline{F}}_1^o = 0 \tag{21.2}$$

$$(\nu_m + j\omega) \underline{\underline{F}}_1^1 - \frac{e}{m} \underline{\underline{E}}_p \frac{\partial F_o^o}{\partial v} - \frac{e}{m} \underline{\underline{B}} \times \underline{\underline{F}}_1^1 = 0.$$

These are the necessary equations[1] for handling breakdown problems, which represent steady state conditions for the electrons. Equations 21.2 are applicable for any orientation of $\underline{\underline{E}}$ and $\underline{\underline{B}}$. We shall consider only those cases in which they are perpendicular or parallel to each other.

Integrating the first expression of Eq. 21.2 over velocity space in spherical coordinates, the second and fourth terms vanish at the limits. The first term gives the total production rate of electrons, $\nu_i n$, from ionization. This is because excitations merely withdraw fast electrons to replace them by slow ones, whereas ionizations add an extra electron. The third term gives the divergence of the flow vector $\underline{\underline{\Gamma}}$

$$\underline{\underline{\Gamma}} = \int_0^\infty \frac{4\pi}{3} \underline{\underline{F}}_1^o v^3 dv \tag{21.3}$$

so that

$$n\nu_i = \nabla \cdot \underline{\underline{\Gamma}} \tag{21.4}$$

Solving the second expression of Eq. 21.2 for $\underline{\underline{F}}_1^o$, we find

1. Allis, Section 24, expecially Eqs. 24.5 to 24.8.

$$\underline{\underline{F}}_1^o = -\frac{v}{\nu_m}\frac{\nu_m^2 + \underline{\underline{\omega}}_b\underline{\underline{\omega}}_b\cdot + \nu_m\underline{\underline{\omega}}_b\times}{\nu_m^2 + \omega_b^2}\nabla F_o^o, \quad \underline{\underline{\omega}}_b = (e/m)\underline{\underline{B}} \tag{21.5}$$

which we substitute in Eq. 21.3 and, assuming that F_o^o can be written as a product $n(x,y,z)f_o(v)$, we find that Γ is proportional to ∇n but not necessarily in the same direction. Accordingly, it is possible to define a diffusion coefficient which is a tensor:

$$\Gamma_i = -\sum_j D_{ij}\frac{\partial n}{\partial j}; \quad i, j = x, y, z. \tag{21.6}$$

If the magnetic field is taken along the z-axis, D_{ij} is given[1] by

$$D_{ij} = \int_0^\infty f_o \begin{bmatrix} \frac{\nu_m}{\nu_m^2+\omega_b^2} & \frac{-\omega_b}{\nu_m^2+\omega_b^2} & 0 \\ \frac{\omega_b}{\nu_m^2+\omega_b^2} & \frac{\nu_m}{\nu_m^2+\omega_b^2} & 0 \\ 0 & 0 & \frac{1}{\nu_m} \end{bmatrix} \frac{4}{3}\pi v^4 dv. \tag{21.7}$$

This expression reduces to the ordinary coefficient $D = \langle v^2/3\nu_m \rangle$ with no magnetic field, $\omega_b = 0$. It is equivalent to Eq. 20.10 except that the present tensor has skew-symmetric terms that were not obtained by the random-walk definition.

Substituting in Eq. 21.4, we obtain the diffusion equation

$$D_{xx}\frac{\partial^2 n}{\partial x^2} + D_{yy}\frac{\partial^2 n}{\partial y^2} + D_{zz}\frac{\partial^2 n}{\partial z^2} + \nu_i n = 0 \tag{21.8}$$

which determines the spatial distribution of the electrons. One can use the normal diffusion coefficient D if lengths are expanded at right angles to the magnetic field in the ratio $\left(\nu_m^2 + \omega_b^2\right)^{1/2}/\nu_m$.

The solution of this equation depends on the boundary conditions. One must define an effective diffusion length Λ_e for the whole cavity which takes into account these expansions:

$$\frac{1}{\Lambda_e^2} = \left(\frac{1}{\Lambda_x^2} + \frac{1}{\Lambda_y^2}\right)\frac{\nu_m^2}{\nu_m^2 + \omega_b^2} + \frac{1}{\Lambda_z^2}. \tag{21.9}$$

The effect of the magnetic field is equivalent to expanding the cavity in the ratio $\left(\nu_m^2 + \omega_b^2\right)^{1/2}/\nu_m$ in all directions perpendicular to the magnetic field.

---

1. Allis, Eqs. 30.3 to 30.7.

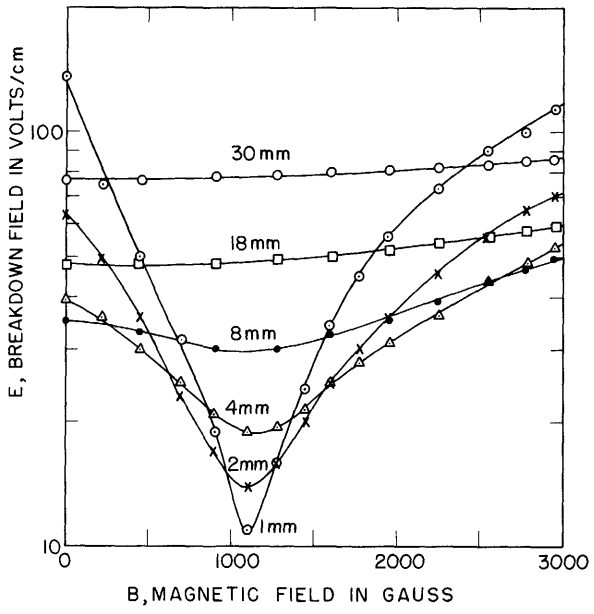

Fig. 16. Breakdown of Heg gas in transverse electric and magnetic field

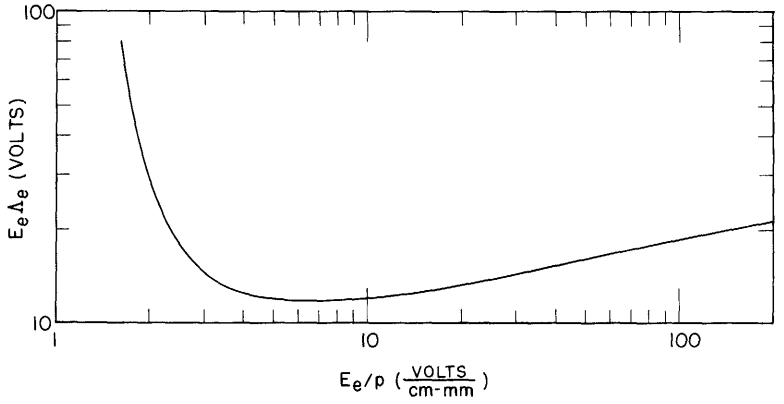

Fig. 17. Theoretical curve for the effective breakdown in Heg gas

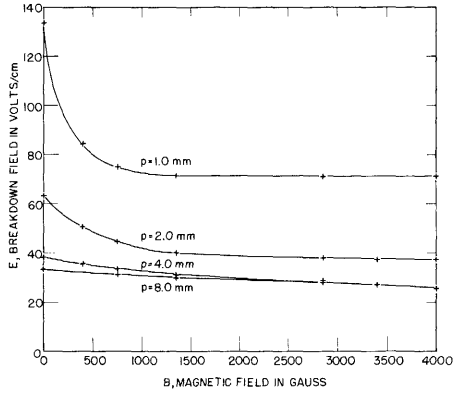

Fig. 18. Breakdown of Heg gas in parallel electric and magnetic fields in a cylindrical cavity. The solid curves are theoretical; the points are experimental

The distribution function F_o^o is obtained by eliminating $\underline{\underline{F}}_1^o$ and $\underline{\underline{F}}_1^1$ from Eqs. 21.2. In this way one obtains Eq. 8.1, in which Λ is replaced by Λ_e, and E by E_e (defined in Eq. 20.14. It follows that all of the breakdown data should plot on a single curve when $E_e\Lambda_e$ is plotted against E_e/p. This is shown in Fig. 17. This exact law is, however, of very limited applicability. The effective quantities E_e and Λ_e depend on ν_m, which is a function of the electron's energy. It is therefore impossible, in general, to make the effective values the same at all of the energies, as the law requires. For helium and hydrogen the collision frequency ν_m is very nearly constant, so that the effective values are significant.

To study the effect of the magnetic field on diffusion alone, the electric and magnetic fields are oriented in the same direction; and in order to reduce diffusion along the magnetic field it is necessary to perform the experiment in a cavity whose height is greater than the radius. In such a cavity the electric field may no longer be considered uniform, and a correction to the computations must be made in a manner shown in Section 16. In the presence of the longitudinal magnetic field the equivalent diffusion length of the cylinder, from Eq. 21.9, is

$$\frac{1}{\Lambda_e^2} = \frac{\nu_m^2}{\nu_m^2 + \omega_b^2}\left(\frac{2.405}{R}\right)^2 + \left(\frac{\pi}{L}\right)^2 . \tag{21.10}$$

Using this and the nonuniform field correction to the Boltzmann theory one obtains the agreement with experiment shown in Fig. 18. This result confirms the predicted effect of the magnetic field upon diffusion.

The breakdown measurements shown in Fig. 16 were made in a flat cavity with the magnetic field transverse to the axis. The effect of the latter is to require the solution of the diffusion equation in an elliptical cylinder whose diffusion length is then given by

$$\frac{1}{\Lambda_e^2} = \frac{\nu_m^2}{\nu_m^2 + \omega_b^2}\left[\left(\frac{\pi}{L}\right)^2 + \frac{1}{2}\left(\frac{2.405}{R}\right)^2\right] + \frac{1}{2}\left(\frac{2.405}{R}\right)^2 . \tag{21.11}$$

Using this and the nonuniform field correction gives the theoretical curves shown in Fig. 19.

B. ELECTRON ATTACHMENT CONTROLLED BREAKDOWN

22. Breakdown in Air

The continuity equation for electrons introduced in Eq. 1.8 can be written in a more general form:

$$\frac{\partial n}{\partial t} = \nu_i n - \nu_e n + S \tag{22.1}$$

where ν_e is any loss mechanism. If, in addition to the diffusion loss, electron attachment is also observed, ν_e, the frequency of loss, may be given as

$$\nu_e n = \nu_a n - D \nabla^2 n, \tag{22.2}$$

where ν_a is the frequency of attachment.

In Eq. 22.1, the external production rate, S, will be considered as introducing a residual electron density n_o, so that the continuity equation becomes

$$\frac{\partial n}{\partial t} = \nu_i n - \left(\nu_a n - D \nabla^2 n\right) \tag{22.3}$$

with the initial condition that at $t = 0$, $n = n_o$.

For those experiments that are available for testing a simple average electron theory of high-frequency breakdown in air, it is a good assumption to take the diffusion as occurring between two parallel plates separated by a distance L. The density configuration is then of the form $\cos(\pi x/L)$, and to a first approximation the term $\nabla^2 n$ can be replaced by $(-\pi^2 n/L)$. Equation 22.3 becomes

$$\frac{\partial n}{\partial t} = \left(\nu_i - \nu_a - \frac{D\pi^2}{L^2}\right) n = \gamma n. \tag{22.4}$$

The solution for Eq. 22.4 is $n = n_o \exp(\gamma t)$. For breakdown, $\gamma = 0$, and

$$\nu_i = \nu_a + \frac{D\pi^2}{L^2}. \tag{22.5}$$

The ionization frequency may be determined from a knowledge of the Townsend first ionization coefficient α, and the ac drift velocity v:

$$\nu_i = \alpha v = \alpha \mu_{dc} E_e, \tag{22.6}$$

where E_e is defined by Eq. 1.3. If $\nu_m^2 >> \omega^2$, E_e is equivalent to the rms value of the high-frequency field. Although the collision frequency may be a function of the average electron energy, an average value of collision frequency may be used as an

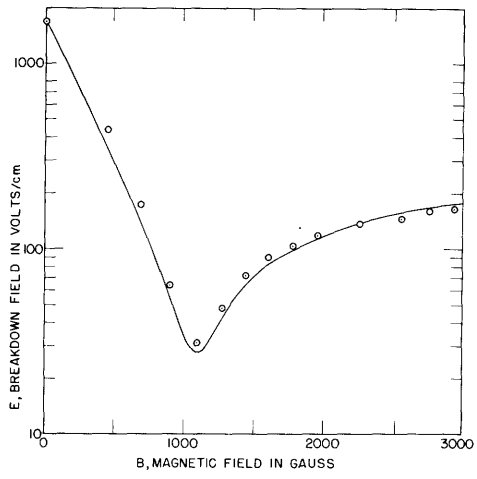

Fig. 19. Breakdown of helium at a pressure of 1 mm Hg in a cylindrical cavity. Solid line is obtained from the Boltzmann theory; points are experimental

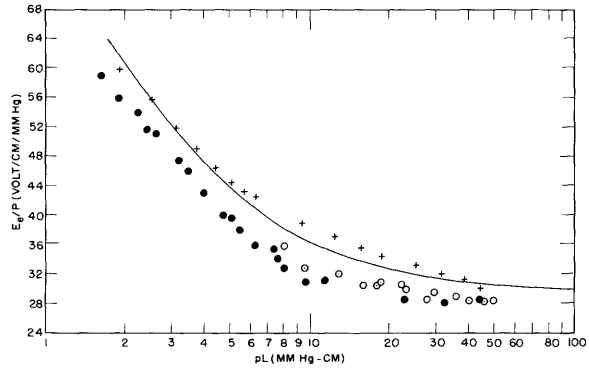

Fig. 20. Breakdown in air.

Solid line, theory
● data of Herlin and Brown
Θ data of Pim
\+ "pure" air

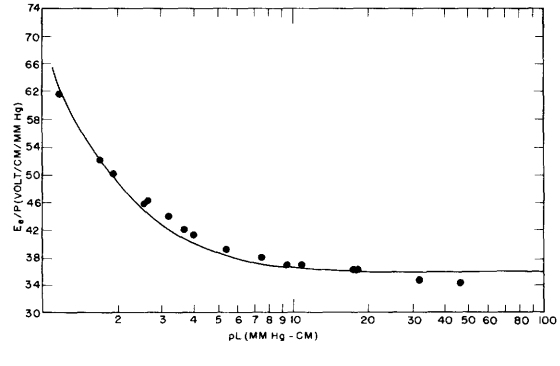

Fig. 21. Breakdown in oxygen. The solid curve is the theory, the points are experimental

approximation. Mobility measurements in air by Nielsen[1], and Riemann[2] may be used to determine μ though the definition of the ac mobility:

$$\mu = \frac{(e/m)\,\nu_m}{\nu_m^2 + \omega^2}.$$

These data yield a value of ν_m for air of $4.3 \times 10^9 p$. The pressure must be greater than 20 mm Hg at a 10-cm wavelength and greater than 70 mm Hg at a 3-cm wavelength in order for the effective field to be equivalent to the rms field.

The attachment frequency may be determined from a knowledge of the number of electrons attached per electron in a path of one centimeter, which is represented by β, and the ac drift velocity. The ratio of the diffusion coefficient to the mobility is given by $(D/\mu) = 2u_{av}/3$ where u_{av} is the average electron energy in electron volts, and the numerical constant depends on the electron distribution function. The value of 2/3 is correct for a Maxwellian velocity distribution.

The condition for breakdown becomes:

$$\frac{\alpha}{p} = \frac{\beta}{p} + \frac{2}{3}\frac{u_{av}\,\pi^2}{(E_e/p)(pL)^2}. \qquad (22.7)$$

The quantities α/p, β/p, and u_{av} are all functions of E_e/p and depend upon the energy distribution function. Measurements of Harrison and Geballe[3] in air yield experimental values of α/p and β/p as a function of E/p. The average electron energy as a function of E/p is given by Healey and Reed.[4]

The solid line in Fig. 20 shows E_e/p as a function of pL as predicted by Eq. 22.7. Measurements of Herlin and Brown[5] at 3000 Mc/sec with the distance varying from 0.635 cm to 0.158 cm and the pressure varying from 70 mm Hg to 2 mm Hg are shown. Measurements of Pim[6] at 200 Mc/sec with the distance varying from 0.08 cm to 0.06 cm and the pressure varying from 760 mm Hg to 160 mm Hg are also given. The experimental results of these observers agree well among themselves but differ from the theoretical curve by as much as 10 per cent. These data were taken by breaking down the gas at the highest pressure possible, for a given set of experimental conditions, reducing the pressure incrementally by pumping, breaking it down again, and so on. Thus, any breakdown products formed at one stage might be present at any subsequent

---

1. R. A. Nielsen, Phys. Rev. 50, 950 (1936).
2. W. Riemann, Z. f. Physik 122, 216 (1944).
3. M. A. Harrison and R. Geballe, Phys. Rev. 91, 1 (1953).
4. R. H. Healey and F. W. Reed, "The Behaviour of Slow Electrons in Gases," Sydney (1941).
5. M. A. Herlin and S. C. Brown, Phys. Rev. 74, 291 (1948).
6. J. A. Pim, Proc. Inst. Elec. Eng. 96, Part III, 117 (1949).

breakdown. The data marked "pure" were taken by introducing fresh air for each measurement. The air was pumped to the desired pressure and only one breakdown initiated. The system was then pumped to 10 μ Hg or below, and the procedure was repeated for the next pressure. Breakdown impurities (such as the oxides of nitrogen) remaining in the gas were thus reduced between readings by a factor of about 10^4. Data collected in this way are shown in Fig. 20 and agree much better with the theory of Eq. 22.7.

23. Breakdown in Oxygen

The breakdown condition of Eq. 22.7 may also be solved for oxygen, since we have the measurement of α/p and β/p for oxygen from the work of Harrison and Geballe.[1] A theoretical plot of E_e/p as a function of pL for O_2 is shown in Fig. 21. Microwave measurements in oxygen at 3000 Mc/sec are also shown, with L = 0.635 cm and over a range of pressures from 70 to 2 mm Hg. In calculating the value of E_e from Eq. 1.5, the value of ν_m was obtained from the mobility measurements of Nielsen and Bradbury[2] and the relation for the ac mobility. This value of ν_m is 3.5×10^9 p.

1. M. A. Harrison and R. Geballe, Phys. Rev. 91, 1 (1953).
2. R. A. Nielsen and N. E. Bradbury, Phys. Rev. 51, 69 (1937).

C. MOBILITY-CONTROLLED BREAKDOWN

24. Behavior of the Average Electron

When the amplitude of the electron oscillation in an electric field is sufficiently high, the electrons can travel completely across the tube and collide with the walls on every half-cycle. If this can occur, the loss of electrons will be controlled by this mobility motion, and the breakdown field will depend upon the amplitude of the electron oscillation[1,2] as given by Eq. 5.8. This equation gave the oscillation amplitude limit for diffusion. On crossing this limit from the diffusion side, a new loss mechanism occurs. The electrons collide with the walls so that the electric field necessary for causing breakdown rises abruptly. This is illustrated[2] in Figs. 22, 23, and 24. Referring to these figures, breakdown to the left of the sharp discontinuities is diffusion-controlled. At that wavelength of the ac field corresponding to the amplitude of oscillation limit for diffusion, electrons are lost by colliding with the walls, and the breakdown field must be sharply increased to make up for this new loss. The breakdown field in the mobility-controlled region is a function of the type of material of which the walls are composed, as we would expect.

In contradistinction to the low-pressure type of secondary emission-controlled breakdown (the electron resonance breakdown, discussed in Chapter D) this high-pressure case is very much a function of the type of gas. This is evident from Eq. 1.2, since the velocity of the oscillating electrons is mobility-controlled, and the mobility is a function of the type of gas. The dependence of the amplitude of oscillation on the electron mobility provides a good substantiation of the factors controlling the critical conditions for crossing the amplitude of oscillation transition. Let us illustrate by taking the case in hydrogen where the drift velocity of electrons is approximately linearly proportional to E/p. This should predict that the critical electric field at the transition value should be proportional to the gas pressure. This is found to be approximately the case by Gill and von Engel, as illustrated in Fig. 25.

One of the most striking characteristics of the mobility-controlled breakdown is the fact that after the electron oscillation amplitude is greater than the tube dimensions -- that is, after all the electrons are lost to the walls -- breakdown is still observed. This is illustrated in Figs. 22 to 24 by the measured breakdown fields on the longer wavelength side of the oscillation amplitude transition. These data also show that the longer the wavelength of the applied ac field, the more easily the discharge starts. The observation that it is such a strong function of the frequency of the electric field requires the effect to be associated with charged particles. The fact that the electrons are being lost

---

1. J. Thompson, Phil. Mag. 23, 1 (1937). S. Githens, Jr., Phys. Rev. 57, 822 (1940).

2. E. W. B. Gill and A. von Engel, Proc. Roy. Soc. 197A, 107 (1949).

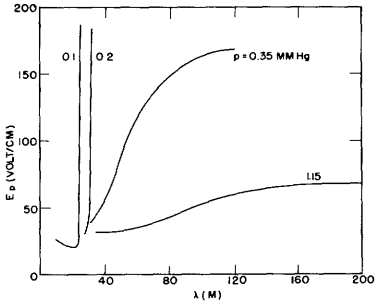

Fig. 22. Breakdown in neon for a flat-ended cylindrical tube 3.55 cm in length

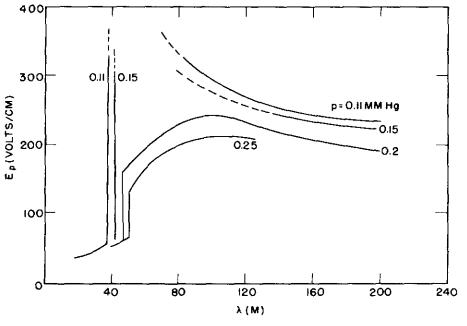

Fig. 23. Breakdown in nitrogen for a flat-ended cylindrical tube 3.55 cm in length

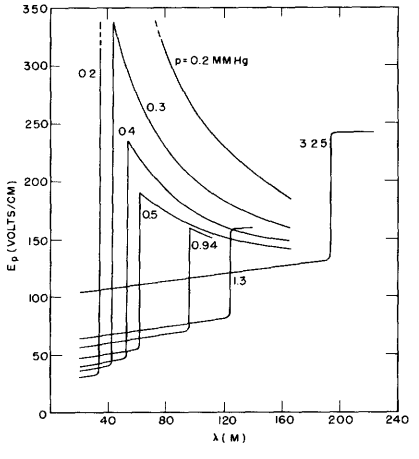

Fig. 24. Breakdown in hydrogen for a flat-ended cylindrical tube 3.55 cm in length

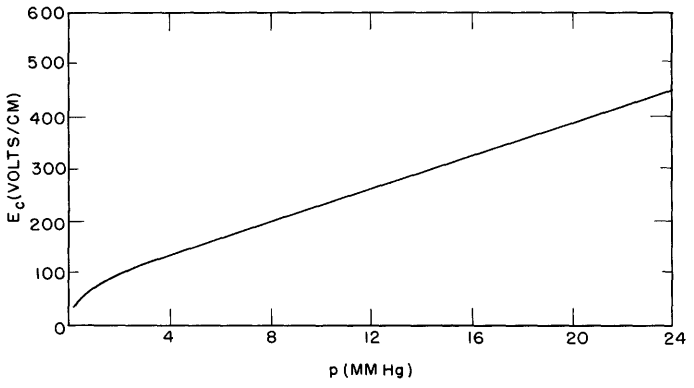

Fig. 25. Cut-off field strength as a function of pressure for hydrogen

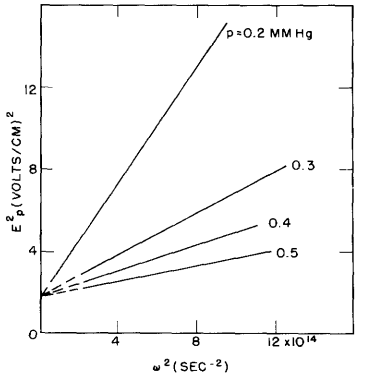

Fig. 26. Relation between field strength and frequency beyond cut-off in hydrogen

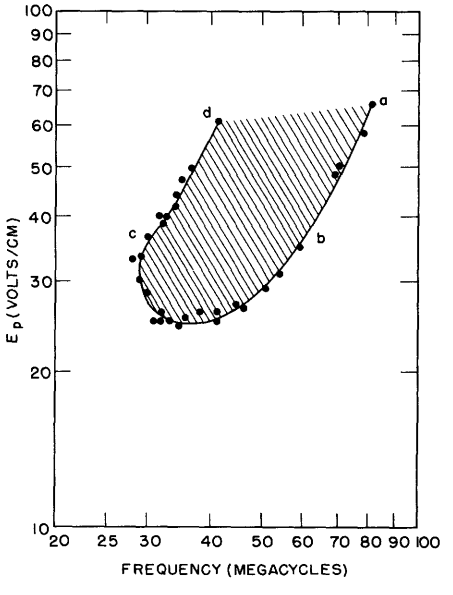

Fig. 27. Breakdown in hydrogen at a pressure less than 0.1 μ Hg

every half-cycle to the walls suggests that the only particles left to account for this increase in ionization must result from the positive ions.

Gill and von Engel used their data in hydrogen to prove that the breakdown beyond the amplitude of oscillation transition was controlled by the positive ion mobility. The amplitude of the oscillation of the velocity obtained from Eq. 1.2 is

$$v_{max} = \frac{eE_p}{m^*\left(\omega^2 + \nu_m^2\right)^{1/2}} = \frac{\sqrt{2}\, eE_e}{m^* \nu_m} \tag{24.1}$$

where m^* is the mass of whatever particle is effective in controlling the discharge. If breakdown occurs when the maximum velocity has reached a constant value v, which is a reasonable assumption when the electrons are produced by secondary emission from the walls, we may write

$$e^2E^2 = (m^*)^2\, v^2\left(\omega^2 + \nu_m^2\right), \tag{24.2}$$

and E^2 plotted against ω^2 should be a straight line. This is illustrated for the data of Gill and von Engel for hydrogen in Fig. 26.

For any pressure, the straight lines are seen to cut the E-axis at a point E_o where $\omega = 0$. Here $eE_o = m^* v\, \nu_m$, but since $(e/m^* \nu_m) = \mu$, the mobility, we have the possibility of identifying the particles by determining what values of e/m^* lead to the correct relation between E and ω at the various pressures measured in Fig. 26. The e/m^* ratio for the molecular hydrogen ion agrees better than one would expect from the elementary nature of the analysis, and leaves little doubt that the ion mobility is the controlling mechanism on the long wavelength side of the oscillation amplitude transition. In this region, therefore, the loss of electrons at the walls resulting from their large oscillation amplitude is more than replaced by the secondary electron emission by positive ion bombardment of the walls, and the breakdown field is shown to decrease as the wavelength increases.

D. SECONDARY ELECTRON RESONANCE BREAKDOWN

25. Behavior of the Average Electron

Many studies have been made of high-frequency breakdown in regions outside that controlled by diffusion. If the pressure is low, the mean free path becomes long compared with the containing vessel, and ionization in the gas becomes highly unlikely. A number of workers have studied this case and have shown that the secondary emission of electrons by direct bombardment of the walls can cause a breakdown to occur. Not only is the magnitude of the electric field important, but the phase of the electron motion with respect to the field has a governing effect. Under optimum conditions, the electron motion must be in phase with the field. Thus, an electron starting across the gap between the walls should collide with the walls and release secondary electrons just as the electric field passes through zero. The reversed electric field accelerates the secondary electrons back across the gap. The electric field must be of such a value that the transit time across the gap shall be equal to one-half cycle of the ac field. In this way the secondary electrons formed by the initial electron become primary electrons for the next half-cycle to form another group of secondary electrons, with the optimum conditions again requiring that the secondaries be formed just as the field reverses its direction.

It is obvious that a breakdown does not require the optimum conditions to occur, and there is a fairly broad region of fields and frequencies over which such a phenomenon may be observed. It should be apparent that for any one frequency, breakdown should be possible in a bounded region between two values of the field corresponding to too little or too much acceleration of the electrons to maintain the proper phase relations.

Because this type of breakdown relies for its electron multiplication on the secondary emission of electrons from the walls, the breakdown field is independent of the type of gas but very dependent on the nature of the walls of the vessel in which the discharge takes place.

With this introduction, let us turn to a more quantitative description of the problem. The motion of an electron acted on by a sinusoidally varying electric field of peak value E_p and radian frequency ω is described by the equation

$$m(dv/dt) = eE_p \sin(\omega t + \phi), \tag{25.1}$$

where ϕ is the phase angle of the secondary-emission electrons, and we here neglect any collision effects between the electrons and gas atoms. For simplicity, let us assume that all electrons have one-half-cycle transit times between the walls and integrate Eq. 25.1 over this half-cycle transit time. We get for the arrival velocity

$$v = v_o + (2eE_p/m\omega) \cos \phi, \tag{25.2}$$

where v_o is the component in the direction of the electric field of the velocity of

emission of the secondary electrons. Integrating again, evaluating over the one-half-cycle transit time, and setting the distance of electron travel equal to the tube wall separation L gives the transit equation

$$L = \pi v_o/\omega + (eE_p/m\omega^2)(\pi \cos\phi + 2 \sin\phi). \tag{25.3}$$

Solving this equation for the electric field, we obtain

$$E_p = \frac{\omega^2 L - \pi v_o \omega}{(e/m)(\pi \cos\phi + 2 \sin\phi)}. \tag{25.4}$$

Let us assume that the ratio between the electron arrival velocity and the electron emission velocity is a constant, $(v/v_o) = k$, so that we may combine Eqs. 25.2 and 25.4 to give

$$v = \left(\frac{k}{k-1}\right) \frac{2eE_p \cos\phi}{m\omega}, \tag{25.5}$$

and

$$E_p = \omega^2 L \Phi^{-1} m/e, \tag{25.6}$$

where

$$\Phi = \frac{k+1}{k-1} \pi \cos\phi + 2 \sin\phi. \tag{25.7}$$

If we combine Eqs. 25.5 and 25.6, writing the velocity in terms of the electron arrival energy u given by $eu = mv^2/2$, we obtain a frequency

$$f = \frac{(k-1)\Phi}{k\pi L \cos\phi} \left(\frac{eu}{8m}\right)^{1/2}. \tag{25.8}$$

Furthermore, for a given experiment at fixed ω and fixed d the minimum electric field in Eq. 25.6 occurs for a maximum Φ. Maximizing Φ with respect to the phase of the emitted electrons, ϕ, gives

$$\phi = \tan^{-1}\left[\left(\frac{k-1}{k+1}\right)\left(\frac{2}{\pi}\right)\right]. \tag{25.9}$$

It is an unfortunate fact that we do not have available the necessary information on the fundamental processes involved in these considerations to substitute values of the parameters in Eqs. 25.6, 25.7, 25.8, and 25.9 to obtain a numerical solution. We therefore have to use them as semiempirical relations to calculate this breakdown region.

Hatch and Williams[1] have made fairly extensive measurements to which we may fit these equations. Their data are shown in Fig. 27. Data on the lower branch of the curve were taken by increasing the electric field strength until breakdown occurred. By suddenly applying a high field and then lowering it slowly, the upper breakdown curve

1. A. J. Hatch and H. B. Williams, J. Appl. Phys. 25, 417 (1954).

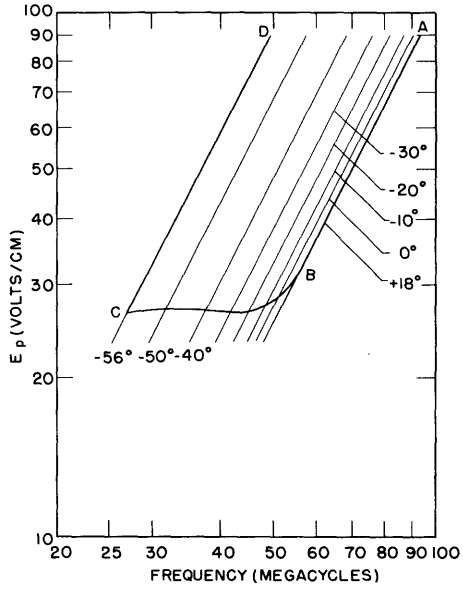

Fig. 28. Theoretical calculation of breakdown for 3-cm electrode separation, minimum electron arrival energy of 60 ev, and k = 3. Various lines represent condition for half-cycle electron transit times at indicated phase angles

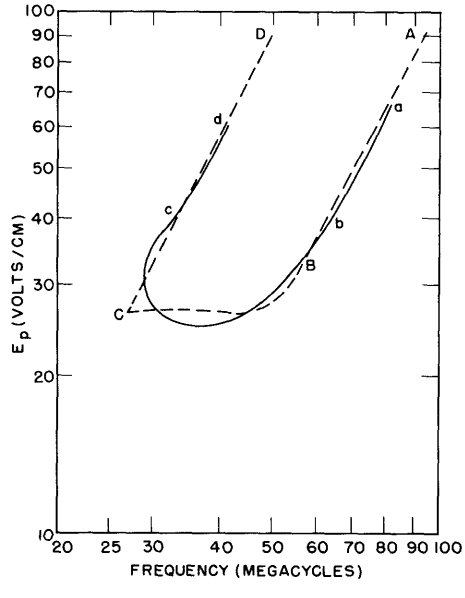

Fig. 29. Comparison of experimental curve of Fig. 27 and theoretical curve of Fig. 28

was observed. Equation 25.6 fits the nearly straight line segment a-b in Fig. 27 when $\phi = 6.6$. Using this empirically fitted value for ϕ in Eqs. 25.7 and 25.9 we find that for this case $k = 3$, $\phi = 18°$. If we continue to assume that k is constant, we may obtain a family of straight lines of slope 2 on a log-log plot of E_p versus frequency for different values of ϕ. Such a plot is shown in Fig. 28. The resonance line A-B for $\phi = 18°$ corresponds to the segment a-b of Fig. 28. The resonance line C-D in Fig. 28 for $\phi = -56°$ corresponds to the segment c-d of Fig. 27.

From Eq. 25.8 a frequency may be determined for each value of ϕ corresponding to a particular electron arrival energy u. The value of the arrival energy which most nearly corresponds to the experimental curve is u = 60 ev. This is the section B-C of Fig. 28. In Fig. 29 are compared the results of this theory with the experimental measurements of Hatch and Williams.

A fair amount of self-consistency is evidenced by the various studies of this type of secondary electron resonance breakdown. Hatch and Williams found $k = 3$, $-56° \leqslant \phi \leqslant 18°$, and u = 60 ev. Danielsson[1] assumed $k = \infty$ ($v_o = 0$), $0° \leqslant \phi \leqslant 90°$, and found u = 80 ev, Henneburg, Orthuber, and Stendel[2] calculated $0° \leqslant \phi \leqslant 32.5°$, assuming zero electron-emission energy. Gill and von Engel[3] found k = 4, u = 90 ev, and the cut-off occurred at $\phi = 58°$. Their treatment did not include a second limiting value of ϕ. These values of k and u are not inconsistent with known secondary electron-emission energies and yields.

Most observers have not taken their data in such a way as to measure the upper branch of the breakdown curve. The common experimental method is to raise the voltage until the tube breaks down at a given frequency. In this case the data take the form shown in Fig. 30, in which the vertical segment of the curve is termed a cut-off. Such a condition corresponds to point C of Fig. 28. This cut-off frequency may be calculated from Eq. 25.8 by using the upper breakdown phase angle Φ_u:

$$f_{co} = \frac{(k-1)\Phi_u}{k\pi L \cos\phi_u} \left(\frac{eu}{8m}\right)^{1/2}. \tag{25.10}$$

For a constant k, ϕ_u, and u, this takes the form

$$f_{co} = (\text{constant})/L, \tag{25.11}$$

where for any particular case the constant may be obtained by fitting to the data.

A collection of measured values for the cut-off frequency, f_{co}, as a function of the reciprocal electrode separations, (1/L) is plotted[4] in Fig. 31. It seems obvious that

---

1. U. Danielsson, Diplomarbeit K. Techn. Hochschule, Stockholm (1943).

2. W. Henneburg, R. Orthuber, and E. Stendel, Z. tech. Phys. 17, 115 (1936).

3. E. W. B. Gill and A. von Engel, Proc. Roy. Soc. 192A, 446 (1948).

4. Other workers cited in this section and C. Gutton, Compt. Rendu 178, 467 (1924); C. Gutton, H. Gutton, Compt. Rendu 186, 303 (1928); H. Gutton, Ann. Phys. 13, 62 (1930).

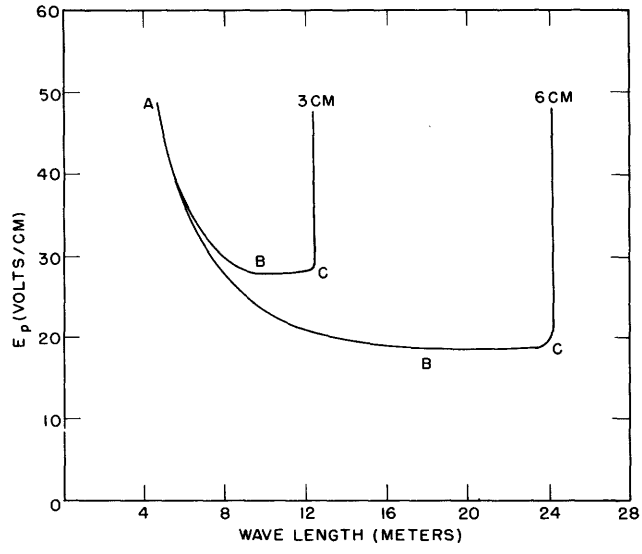

Fig. 30. Breakdown field strength as a function of wavelength for flat-ended cylindrical tubes 3 cm and 6 cm long with axes parallel to the field for hydrogen at a pressure of 1 μ Hg

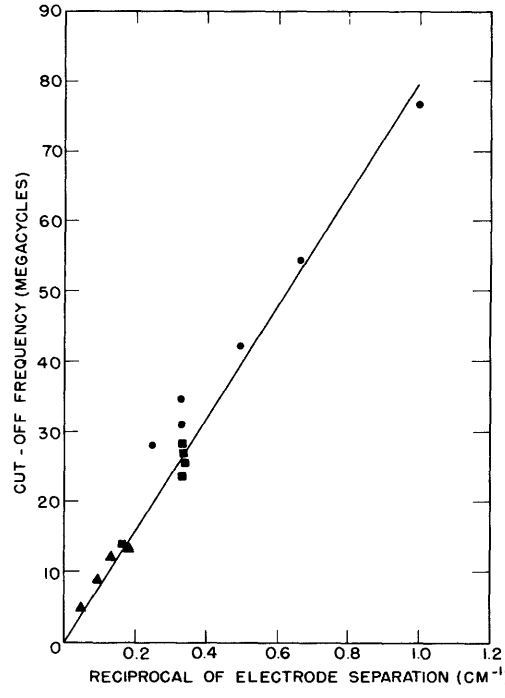

Fig. 31. Summary of cut-off frequencies versus reciprocal electron separation from data of several observers.

▲ Gutton
■ Gill and von Engel
● Hatch and Williams
Solid line, cut-off law, $f_{co} = 79/L$

Eq. 25.11 is verified by these data.

The breakdown voltage at cut-off is

$$V_{co} = \frac{u(k-1)^2 \Phi_u}{2k^2 \cos^2 \phi_u} . \qquad (25.12)$$

Thus the breakdown voltage at cut-off is independent of electrode separation and applied frequency. For fixed k and ϕ_u, Eq. 25.12 may be written as

$$V_{co} = (\text{constant})\, u \qquad (25.13)$$

where the constant may be determined empirically.

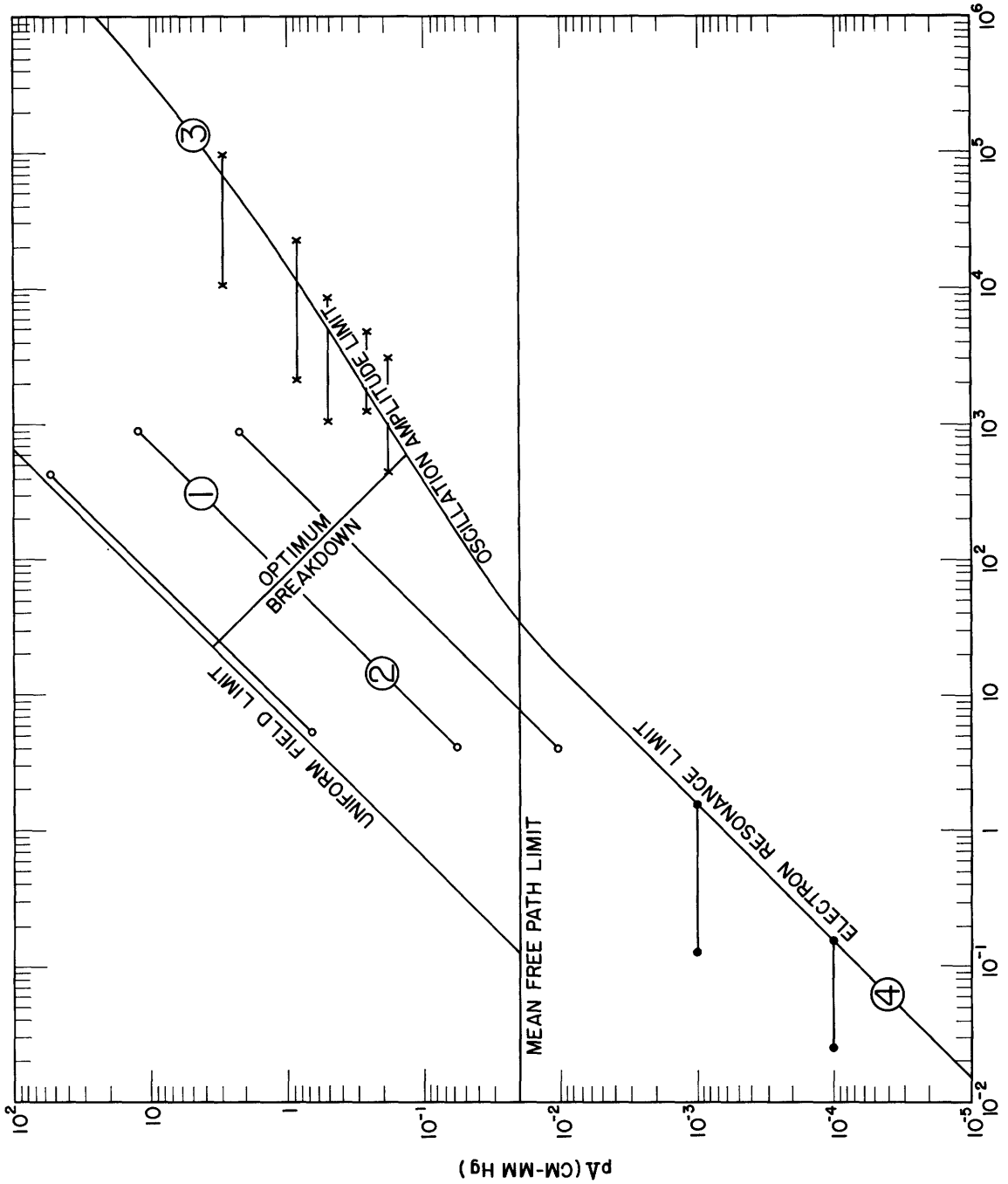

Fig. 32. Summary of the regions of high-frequency breakdown on the pΛ-pλ plane

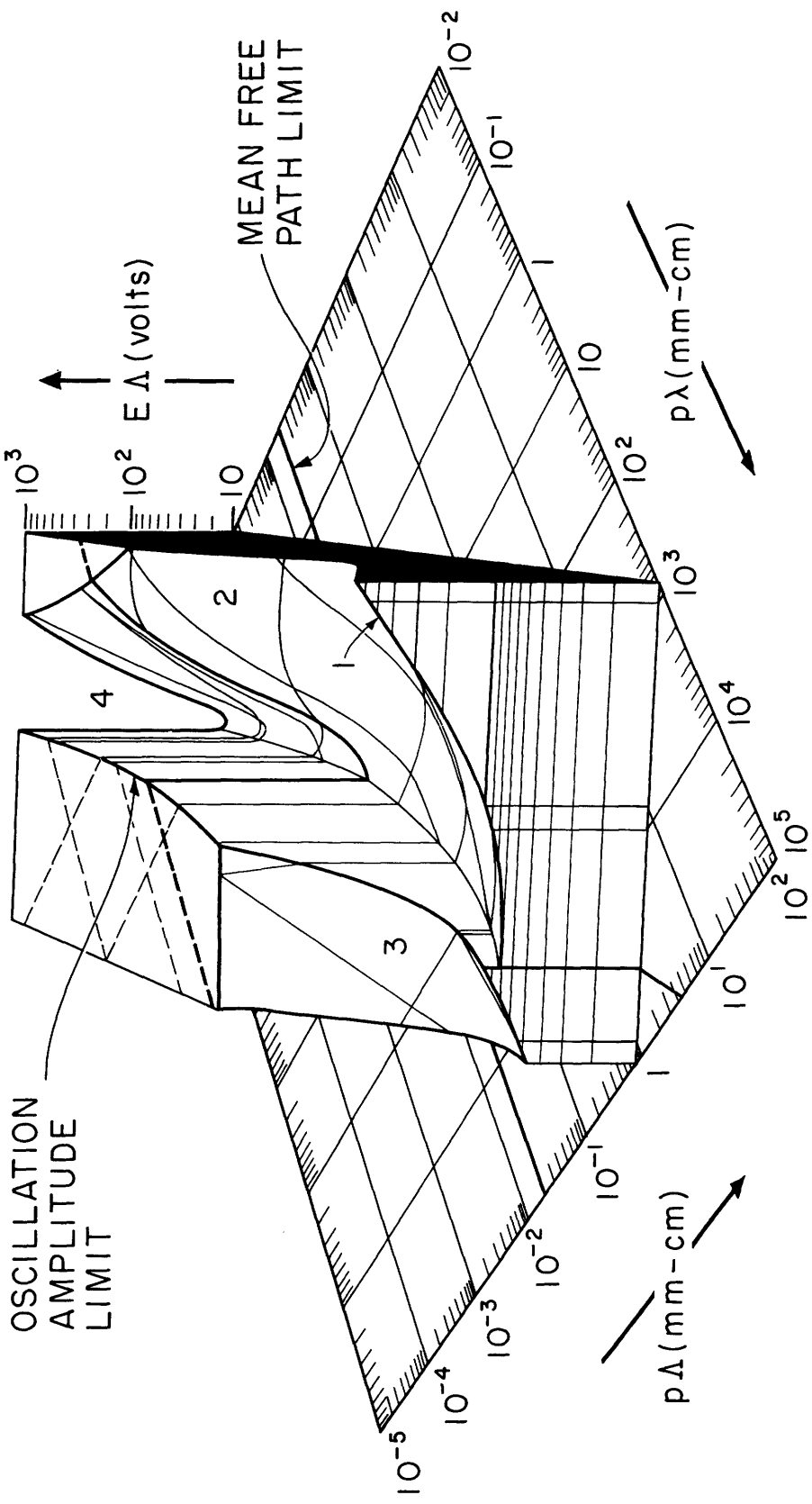

Fig. 33. Summary of the regions of high-frequency breakdown on the pΛ-pλ-EΛ surface

E. SUMMARY OF HIGH-FREQUENCY BREAKDOWN MECHANISMS

26. The $p\Lambda$-$p\lambda$ Plane

Many experimenters have studied the breakdown of a gas discharge at various frequencies and in various different geometrical arrangements. Most workers have obtained breakdown data in hydrogen and several have included in their reports sufficient detail for determining the parameters p, λ, and Λ. When these parameters are known, the data may be plotted in the $p\Lambda$-$p\lambda$ plane of Fig. 3. Two general experimental methods of collecting data have been used. The breakdown measurements reported in Chapter A were taken with the frequency constant with a given electrode separation and with a varying pressure. Such a technique results in data in which a single run would plot as a line at 45° on the $p\Lambda$-$p\lambda$ plane. The extent of the measurements taken in hydrogen, presented in Chapter A, are plotted in this way in Fig. 32. The breakdown curves reproduced in Chapters C and D were taken by varying the frequency at a given pressure and electrode separation. These data will therefore plot as horizontal lines on the $p\Lambda$-$p\lambda$ plane, and the measurements discussed in Chapters C and D are thus indicated on Fig. 32. It is clear from this figure that data exist which cross the various limits and regions discussed throughout this entire article, and it is therefore important to correlate the data of various workers to determine whether or not, for a single gas, an over-all picture may be arrived at.

27. The $p\Lambda$-$p\lambda$-$E\Lambda$ Surface

In our discussion of proper variables in Section 4 we arrived at the variables $p\Lambda$, $p\lambda$, and $E\Lambda$ from dimensional analysis considerations, and therefore these variables should not be restricted to any particular breakdown mechanism. All breakdown data taken for a given gas should fall in a single $p\Lambda$-$p\lambda$-$E\Lambda$ surface. This is shown for hydrogen in Fig. 33, constructed from the actual data reported in the literature. Not only do all of the data fall on a single surface, but insofar as the work of different experimenters overlaps on the illustrated surface, their measurements agree within the accuracy of drawing such a model.

Figure 33 has been drawn to summarize the sections of this article. Regions 1 and 2 were discussed in Chapter A, particularly in Sections 3 and 12. Region 1 corresponds to the high-pressure data for hydrogen illustrated in Fig. 2. In Region 2 the effective field defined by Eq. 1.5 is significant. The rising curve along the optimum breakdown line for increasing Λ results, for example, from the nonuniform field effects discussed in Section 16, and illustrated in Fig. 11. Region 3 is described in Chapter C; Region 4, in Chapter D.

A similar $p\Lambda$-$p\lambda$-$E\Lambda$ surface could be drawn for different gases and for the superimposed dc and magnetic field of Sections c and d by substituting for the geometrical Λ the appropriate effective Λ discussed in these sections.